

# Scoping Assessment of Erosion Levels for the Mahale region, Lake Tanganyika, Tanzania

August 2015

## **Authors**

J.E. Hunink

W. Terink

S. Contreras

P. Droogers

## **Client**

The Nature Conservancy (TNC)

**Report FutureWater: 148**



## **FutureWater**

Costerweg 1V  
6702 AA Wageningen  
The Netherlands

+31 (0)317 460050

[info@futurewater.nl](mailto:info@futurewater.nl)

[www.futurewater.nl](http://www.futurewater.nl)

# Preface

The Nature Conservancy (TNC) launched with several partners the Tuungane project that aims to reduce threats to biodiversity conservation and natural resources degradation in the Greater Mahale Ecosystem, while simultaneously improving health of the communities. Increased erosion and sedimentation are a key threat in the region arising from reduction of the vegetative cover and non-sustainable land management practices. Farming, grazing, and dry-season burning contributes to the erosion hazard with severe impacts on the fish habitats, affecting the environment and the coastal communities.

This study aims to quantify the erosion hazard in the area, better understand its link with land use and management, and take a first step in building a roadmap towards more sustainable land management of the Mahale region. The analysis is based on erosion modeling, using state-of-the-art tools and high-resolution spatial datasets in collaboration with TNC.



## Summary

This report summarizes the erosion modeling assessment of several pilot watersheds of the Mahale region in the Lake Tanganyika basin, Tanzania. The hydrological model SPHY (Spatial Processes in Hydrology) was applied using the sediment module that is based on the MUSLE approach, to assess hydrological flows, erosion and sediment yield on a high spatial and temporal resolution. This allowed the analysis of the spatial and temporal variability of the erosion hazard, and a better understanding of the relationships between erosion and land use and management. Also a preliminary assessment of priority areas for interventions was carried out.

The analysis highlights several key factors for erosion and options for mitigation in the study area. The differences in the area in protection status, wildfire frequency and rainfall cause a very high variability in vegetative cover. This explains to a large extent the erosion susceptibility in the area. Mitigation measures should focus on these areas, especially on steeper slopes. Also, in the light of climate change, it is recommended to increase the understanding of the high rainfall variability in the region.



# Table of contents

<b>1</b>	<b>Introduction</b>	<b>7</b>
1.1	Background	7
1.2	Erosion sources	8
1.3	Erosion impacts	9
1.4	Objectives	10
<b>2</b>	<b>Methods</b>	<b>12</b>
2.1	Biophysical setting	12
2.2	Overall approach to assessment	13
2.3	Modelling specifications	13
	2.3.1 Hydrology	13
	2.3.2 Erosion modelling	15
2.4	Input datasets	16
	2.4.1 Overview of datasets used	16
	2.4.2 Elevation	17
	2.4.3 Rainfall	18
	2.4.4 Evapotranspiration	21
	2.4.5 Soil properties	22
	2.4.6 Soil erodibility	23
	2.4.7 Land use and land cover change	24
	2.4.8 Wildfire	26
	2.4.9 Crop management and practices	28
<b>3</b>	<b>Results</b>	<b>30</b>
3.1	Spatial analysis of runoff and erosion	30
3.2	Sediment yield into Lake Tanganyika	35
3.3	Land use and management	32
3.4	Preliminary selection of priority areas	35
<b>4</b>	<b>Conclusions</b>	<b>41</b>
4.1	Main findings and recommendations	41
4.2	Potential future analysis steps	42
<b>6</b>	<b>References</b>	<b>44</b>



## Tables

Table 1. Overview table of rainfall data.....	18
Table 2. Crop factors for each land cover .....	22
Table 3. Total area and relative share of each land use class based on map in Figure 14. ....	25
Table 4. Crops cultivated by farmers according to the socio-economic survey in 2011 in the area (source: TNC).....	26
Table 5. Sediment yield, average fire return interval and average slope for the land use types in the area .....	33
Table 5. Total area, sediment yield, average slope and drainage area for recently converted agriculture compared to agricultural area that is cultivated for a longer time ....	<b>Error! Bookmark not defined.</b>

## Figures

Figure 1. Two key terrestrial ecosystems in the Tuungane project area: humid mountainous evergreen forest (left), and sub-humid miombo forest (right).....	7
Figure 2. Burned area in bamboo/Miombo zone in study area (left, source: Google Earth) and burned Miombo woodland on steep slope (right) .....	8
Figure 3. Erosion patterns based on regional erosion modeling (source [Drake et al., 1999]).....	9
Figure 4. Changes in the fish population for study site in Lake Tanganyika over a 20-year period (source: [Takeuchi et al., 2010]).....	10
Figure 5. Pilot watersheds for this study within the Greater Mahale Ecosystem (source: TNC)	12
Figure 6: SPHY model conceptual diagram.....	15
Figure 7. Spatial distribution of the topographic USLE factor (LS) .....	17
Figure 8. Spatial distribution of the time of concentration (hr) .....	18
Figure 9. Locations of the rainfall gauges – in pink the border of the study area .....	19
Figure 10. Average satellite-based vegetation greenness index (NDVI from MODIS MID13A2)	20
Figure 11. Mean annual rainfall distribution from daily FEWS data.....	21
Figure 12. Average monthly rainfall for entire study area from daily FEWS data .....	21
Figure 13. Two soil parameters (left: clay percentage, right: saturated hydraulic conductivity) extracted from SoilGrids.....	23
Figure 13. Spatial distribution of the soil erodibility factor (K) .....	24
Figure 14. Land use map for the study area. The modeling domain corresponds to the area delimited with the pink line. ....	25
Figure 15. Land conversion to agriculture (source: TNC) .....	26
Figure 16. Fire return interval for the study area.....	27
Figure 17. Aboveground tree carbon stock against fire return interval for three fire intensity classes (source [Ryan and Williams, 2011]) .....	28
Figure 18. Spatial distribution of USLE crop management factor .....	29
Figure 19. Principal catchments in the study area .....	30
Figure 20. Mean annual runoff (left) and mean annual erosion rate (right). ....	31
Figure 21. Annual sediment yield (tons/cell) against slope (-), mean annual rainfall (mm), runoff (mm), and elevation (masl).....	32
Figure 22. Annual erosion during a relatively dry year (2003, left) and a wet year (2009, right).	32
Figure 23. Monthly runoff and baseflow regime for 4 selected catchments in the area, starting in middle of dry season .....	36



Figure 24. Mean annual sediment yield (tons/yr) for each catchment in the area ..... 36  
Figure 25. Average daily sediment yield (tons/day) for 4 selected catchments in the area..... 38  
Figure 26. Specific yield (ton/ha) and total sediment yield per land use class, based on 10-year average..... 33  
Figure 27. Fire return interval and erosion for three land use classes affected by wildfires ..... 35  
Figure 28. Preliminary map of priority areas based on the erosion modeling assessment ..... 39



# 1 Introduction

## 1.1 Background

The world's longest lake, Tanganyika, holds 17 percent of our planet's fresh surface water and boasts more than 300 fish species. The Greater Mahale Ecosystem encompasses 4.8 million acres of mostly forested landscape and is home to approximately 93 percent of Tanzania's 2,800 endangered chimpanzees. Local communities of small-scale farmers and fishers still live close to the land, and their lives and livelihoods are dependent upon the area's rich natural resources.

The health of this diverse natural environment and the well-being of its people are threatened by extreme poverty compounded by a rapidly growing human population. For this reason, TNC and several partners have started in 2013 the Tuungane Project: Uniting People and Nature. The goal of the project is to provide to remote villages better access to health services and education to achieve a more sustainable use by the population of the natural resources.

Land use change over the last decades has caused forest to be cleared for agriculture, and erosion is considered an increasing problem in the watersheds draining to Lake Tanganyika for the loss of fertility upstream but more important for its impact on the fish habitat in the Lake [Maruyama *et al.*, 2011]. Sedimentation is likely one of the principal causes of the declined fisheries in the coastal zones [Van Steenberge *et al.*, 2011] with its negative consequences on the local communities.

The overall goal of the Tuungane project is to reduce threats and improve the resilience of this system and to bring together reproductive-health and conservation interventions to reduce the pressures on people and nature.



**Figure 1. Two key terrestrial ecosystems in the Tuungane project area: humid mountainous evergreen forest (left), and sub-humid miombo forest (right)**

## 1.2 Erosion sources

The Lake Tanganyika basin is shared by four countries: Rwanda, D.R. of Congo, Zambia and Tanzania. Increased human-induced erosion in the basin started in the 18<sup>th</sup> century, but in Tanzania, extensive watershed deforestation started only in early-20<sup>th</sup> century [Cohen *et al.*, 2005], principally because of mining [Conaway *et al.*, 2012; Odigie *et al.*, 2014] and human settling. Currently, erosion in this area is linked mainly to uncontrolled dry season fire activity, the use of fire in land clearance and the usage of fire for cooking and charcoal production [Palacios-Fest *et al.*, 2005].



**Figure 2. Burned area in bamboo/Miombo zone in study area (left, source: Google Earth) and burned Miombo woodland on steep slope (right)**

Several studies have been carried out on the impacts of increased sediment inputs into the lake (discussed afterwards) but few studies have been done on the sources of erosion in this area. So far, the biggest effort took place by a large group of researchers in a project funded by the United Nations Development Programme/Global Environment Facility starting in 1998 on sediment discharge and its consequences in the Lake Tanganyika basin [Patterson, 2000].

One of the conclusions of the former project [Patterson, 2000] was that there is a lack of long-term monitoring data which could have been used to monitor changes of the dynamics of suspended sediments. During this project, some streams of the Lake Tanganyika basin were monitored but this monitoring effort has not continued.

This same study comes to the conclusion that there is strong evidence of large increases of suspended solids entering the lake compared to historical rates of input. This study relates this to a combination of woodland clearances and agricultural practices carried out in the catchment [Patterson, 2000].



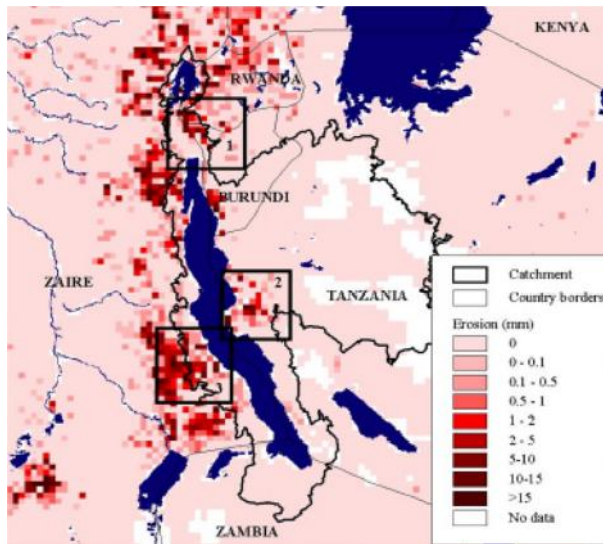


**Figure 3. Erosion patterns based on regional erosion modeling (source [Drake et al., 1999])**

Again within the same project, Nkotagu and Mbwambo [1999] compared streams from two similar-sized adjacent catchments in Tanzania: the Mitumba, forested and protected (in Gombe Stream National Park), and the Ngonya, an impacted catchment, colonized and cultivated by people. The impacted catchment Ngonya showed an order of magnitude greater suspended sediment load than the Mitumba in the protected catchment. Clay minerals were the dominant component of the suspended sediment load [West, 2001]. Eggermont and Verschuren [2003] suggest that inputs into the lake by coarsely-textured sediments have increased, at the expense of the soft-bottom, organic muds which characterise the natural deep-water environment.

Also a soil erosion modelling assessment was carried out [Drake et al., 1999] within the context of an UNDP project. The researchers assessed regional erosion patterns of the entire basin, for one particular season. They assessed priority areas and identified the Mahale region (zone 2 in Figure 3) as one of the critical areas.

Cohen et al. [2005] stress that differences in sediment yield and thus lake floor distribution of that yield are linked to factors such as watershed size, slope, and sediment retention, and must be accounted for in watershed management plans. They were able to link high extreme rainfall events in the 1960-s with increased lake floor sediment accumulation, thus highlighting the importance of the rainfall and runoff regime.

### 1.3 Erosion impacts

Erosion can have a large impact on the soil quality and thus land productivity. Erosion removes valuable top soil which is the most productive part of the soil profile for agricultural purposes. The loss of this top soil results in lower yields and higher production costs. When top soil is gone, erosion can cause rills and gullies that make the cultivation of paddocks impossible. Typical examples are (i) reduced ability of the soil to store water and nutrients; (ii) exposure of subsoil, which often has poor physical and chemical properties; (iii) higher rates of runoff, shedding water and nutrients otherwise used for crop growth; and (iv) loss of newly planted crops



Besides those local impacts, erosion causes sediment loads into downstream areas, streams and lakes. Several researchers have studied pervasive impacts on the aquatic ecosystem of erosion and the resulting increased sediment inputs into lakes [Donohue and Garcia Molinos, 2009]. By modifying both bottom-up and top-down ecological processes and restructuring energy flow pathways, increased sediment loads not only alter biotic assemblage structure and ecological functioning significantly, but frequently result in reduced biological diversity and productivity, as for example Van Boxclaeer et al. demonstrated for Lake Tanganyika [2012].

Eggermont and Verschuren [2003] studied species diversity of Lake Tanganyika and relations with particle size. They found that sediment pollution negatively impacts the oxygenated deep-water environment of Lake Tanganyika, and that intensifying soil erosion in tributary drainages may eventually threaten the survival of endemic species dependent on the habitat it provides. Takeuchi et al. [2010] studied tropical fish communities for several sites in Lake Tanganyika over a 20-year period and observed reductions that they related to human impacts on food conditions (Figure 4).

Impacts of increased run-off and sediment inputs and on habitat heterogeneity, foraging opportunities and food quality for deep-water animals have also been studied by for Lake Tanganyika by McIntyre [2005] for the southern regions of Lake Malawi [Otu et al., 2011], and the Lugu Lake SW China [Zhang et al., 2013]. Increased sedimentation, together with increasing lake temperatures and reduced nutrient inputs due to fires, can important implications for the productivity Lake Tanganyika fishery [Tierney et al., 2010].

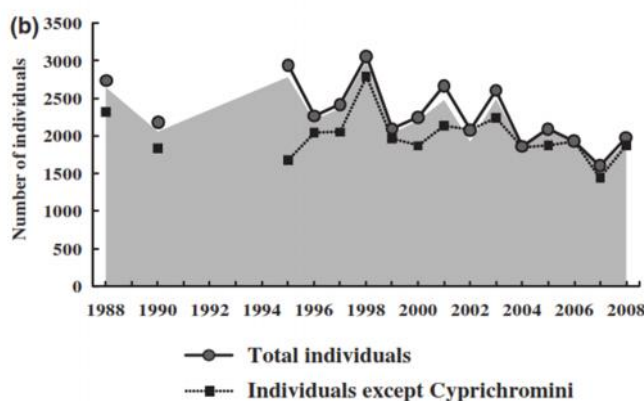


**Figure 4. Changes in the fish population for study site in Lake Tanganyika over a 20-year period (source: [Takeuchi et al., 2010])**

The distance that sediments are transported is influenced by the seasonal flow regime of the river tributaries and the topography of the lakeshore close to the river mouth. Sediment can be transported in significant quantities at least 10 km from source, depending on streamflows and sediment texture. Its impact is most likely higher where rivers discharge into relatively gently-sloping lake floors [Patterson, 2000].

## 1.4 Objectives

The Nature Conservancy is currently preparing a Blueprint for the Lake Tanganyika system that should provide comprehensive insight in the interactions between people and nature in this region, and links between upstream land use and the lake ecosystem. Within this effort, it is necessary to obtain a better understanding of the erosion and sediment yields that are related



to changing land use patterns in the watersheds draining to the lake. This assessment should enable a better design of the activities with the communities in the upstream areas to promote sustainable land use management practices. It should also provide the input for a subsequent analysis on the potential threats to the fish communities in the lake.

The purpose of this study is to support TNC in its effort in a first level scoping assessment on erosion levels in the Tuungane project area. Erosion and hydrological modelling is carried out to assess erosion patterns in a number of pilot erosion modelling watersheds (Figure 5) and determine the relations between sediment yields and land use. This scoping modeling study is carried out using gathered data from a wide range of sources, and previous research.

The specific objectives for the assignment are:

- Provide a first level assessment of the erosion and sediment yield levels of selected priority watersheds in the project area
- Analyze spatial patterns and its relation with land use management
- Obtain an estimate of the range in temporal variability in sediment yield entering the lake.
- Outline and advise on further activities in terms of more details, expansion to other watersheds and potential interventions.



### 2.1 Biophysical setting

The study area concerns the Mahale region which includes the Mahale Mountains National Park, and several surrounding watersheds draining to Lake Tanganyika (Figure 5). The terrain is mostly rugged and hilly and is dominated by the Mahale Mountains chain in the northwestern part of the study area. The highest peak is Nkungwe that rises 2,462 m above sea level.

The area is sub-humid to humid, characterized by one long rainy season that begins in early October, followed by a relatively short dry season that begins in the middle of May. The area receives around 1000 mm of rainfall per year. Some small parts of the area receive more rainfall due to orographic lift of moist air.

The main land cover types are evergreen medium-altitude forest, montane forest, Miombo woodland, and *Oxytenanthera* bamboo woodland. The Miombo woodland is sparsely populated and economic activities include cattle rearing and hunting. The coastal zone has a few locations with paddy farming, and cassava, maize, beans and oil palm are grown. The main economic activity is fishing.



Figure 5. Pilot watersheds for this study within the Greater Mahale Ecosystem (source: TNC)



## 2.2 Overall approach to assessment

Spatial erosion assessment models can be distinguished among those that are static and dynamic. Static or steady-state models do not concern themselves with the time factor. Dynamic models consider time as an independent variable and can compute the time variability of erosion and sediment yields.

Advantages of using steady-state models are their straightforwardness and low data requirements, providing a qualitative measure of erosion risk. The main disadvantage of using static index-based methods is that the high seasonal and inter-annual variability in climate conditions is not taken into account, resulting often in erroneous results. This can be very relevant in areas where a large variability exists in rainfall conditions and thus in hydrological and sediment fluxes. For example, extreme rainfall events in 1961-62 have been linked in the study area with sediment accumulated in the lake [Cohen *et al.*, 2005].

Also, for this particular study, a dynamic approach is preferable in order to obtain a quantitative estimate of the range in variability of water and sediment yield input into the Lake: this variability will determine to a high level how fish habitats are impacted (dispersion and accumulation of sediments), as demonstrated by several researchers in the Lake Tanganyika [Eggermont and Verschuren, 2003; McIntyre *et al.*, 2005].

One of the most widely applied empirical models for assessing erosion is the Universal Soil Loss Equation (USLE), developed by Wischmeier and Smith in 1978. This model takes into consideration several determining factors, such as the soil erodibility, rainfall intensity, slope length and steepness, land cover and management and agricultural practices.

The MUSLE is a modified version of the famous USLE equation, developed by the U.S. Department of Agriculture (USDA) Soil Conservation Service. It is used in several advanced hydrological modeling as for example the Soil and Water Assessment Tool (SWAT). While USLE predicts sediment yield as function of rainfall, the MUSLE equation takes into account the actual runoff generated that depends on soil moisture.

To be able to use the MUSLE approach, a hydrological model needs to be applied and set up to assess the variability in runoff generation across the landscape. FutureWater with several international partners has developed a hydrological model called SPHY (Spatial Processes in Hydrology, [www.sphy-model.org](http://www.sphy-model.org)). This model includes a module that calculates based on rasterized and dynamic input datasets of climate, soil and land use management the erosion and sediment yield levels, using the MUSLE equation. More details on the SPHY model and erosion modeling are found in the following sections.

The SPHY model was set-up for this study with a spatial resolution of 250x250m. The total modeling domain is 6,916 km<sup>2</sup>, leading to 110,658 calculation cells. The simulation time step is daily and the model was set up for a 10 year period (2001-2010).

## 2.3 Modelling specifications

### 2.3.1 Hydrology

The SPHY (Spatial Processes in Hydrology) model is a hydrological modeling tool suitable and applied for a wide range of water resource management applications. It is a state-of-the-art,



easy to use, robust tool, that can be applied for operational as well as strategic decision support. The SPHY modeling package is available in the public domain and is open-source. SPHY is developed by FutureWater in cooperation with national and international clients and partners and is meant to close the gap between the more complex hydrological models and the steady-state approaches.

The SPHY model has been applied and tested in various studies ranging from real-time soil moisture predictions in flat lands, to operational reservoir inflow forecasting applications in mountainous catchments, irrigation scenarios in the Nile Basin, and detailed climate change impact studies in the snow- and glacier-melt dominated the Himalayan region. Detailed information can be found at the SPHY website ([www.sphy.nl](http://www.sphy.nl))

SPHY was developed with the explicit aim to simulate terrestrial hydrology at flexible scales, under various land use and climate conditions. SPHY is a spatially distributed leaky bucket type of model, and is applied on a cell-by-cell basis. In order to minimize the number of input parameters, and avoid complexity and long model run-times, SPHY does not include energy balance calculations, and is therefore a water-balance based model. The main terrestrial hydrological processes are described in a physically consistent way so that changes in storages and fluxes can be assessed adequately over time and space. SPHY is written in the Python programming language using the PCRaster dynamic modelling framework.

An overview of the SPHY model concepts is shown in Figure 6. SPHY is grid-based and cell values represent averages over a cell, but sub-grid variability is taken into account. The land compartment is divided in two upper soil stores and a third groundwater store, with their corresponding drainage components: surface runoff, lateral flow and base flow. Any precipitation that falls on land surface can be intercepted by vegetation and in part or in whole evaporated. The snow storage is updated with snow accumulation and/or snow melt. A part of the liquid precipitation is transformed in surface runoff, whereas the remainder infiltrates into the soil. The resulting soil moisture is subject to evapotranspiration, depending on the soil properties and fractional vegetation cover, while the remainder contributes in the long-term to river discharge by means of lateral flow from the first soil layer, and base flow from the groundwater reservoir.

As input SPHY requires data on state variables as well as dynamic variables. For the state variables the most relevant are: Digital Elevation Model (DEM), land use type, glacier cover, reservoirs and soil characteristics. The main dynamic variables are climate data such as precipitation, temperature, reference evapotranspiration. Since SPHY is grid-based optimal use of remote sensing data and global data sources can be made. For example, the Normalized Difference Vegetation Index (NDVI) can be used to determine the Leaf Area Index (LAI) in order to estimate the growth-stage of land cover. For setting-up the model data on streamflows are not necessary. However, to undertake a proper calibration and validation procedure flow data are required. The model could also be calibrated using actual evapotranspiration, soil moisture contents, or snow coverage.



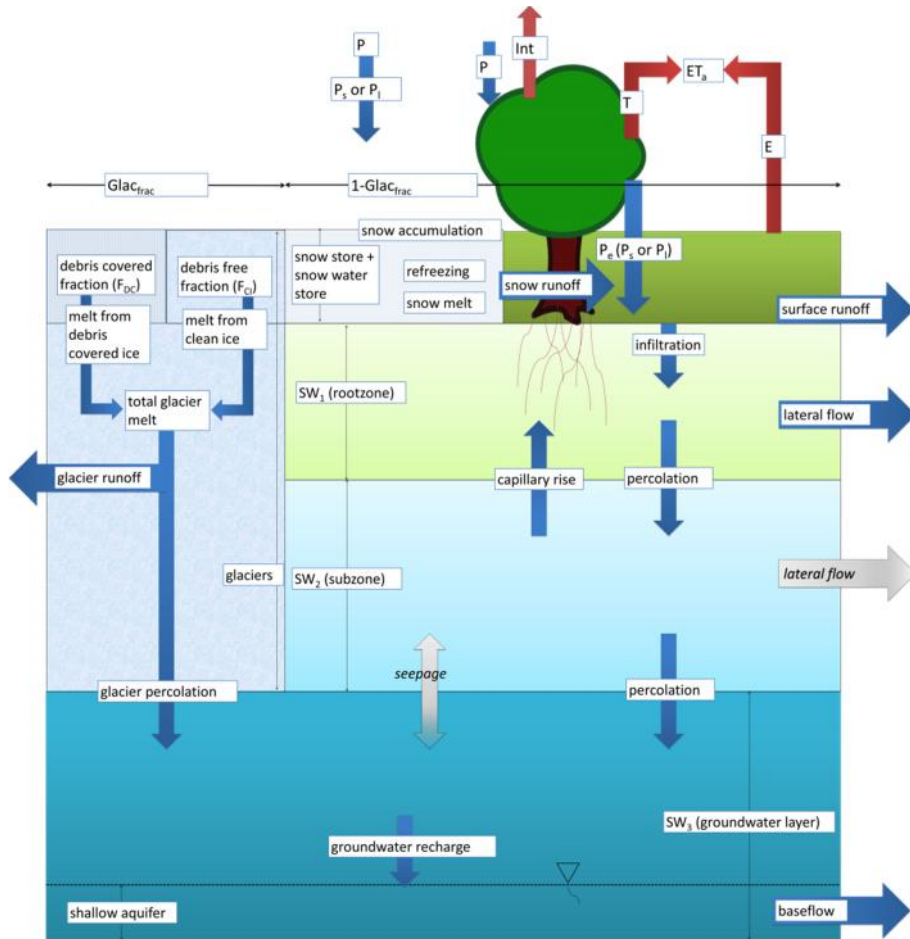


**Figure 6: SPHY model conceptual diagram.**

The SPHY model provides a wealth of output data that can be selected based on the preference of the user. Spatial output can be presented as maps of all the hydrological processes. Maps often displayed as output include actual evapotranspiration, runoff generation (separated by its contributors), and groundwater recharge. These maps can be generated on daily base, but most users prefer to get those at monthly or annual aggregated time periods. Time-series can be generated for each location in the study area. Time-series often used are stream flow under current and future conditions, actual evapotranspiration and recharge to the groundwater.

### 2.3.2 Erosion modelling

The Universal Soil Loss Equation (USLE) is the method most commonly used to estimate long-term erosion rates from field or farm sites that are subject to different management practices. Wischmeier and Smith [1978] developed the method based on data from many experimental plots in the USA, but the method has been applied and argued globally [Wischmeier, 1976; Sonneveld and Nearing, 2003].

The SPHY model estimates erosion and sediment yield with the Modified Universal Soil Loss Equation (MUSLE) [Williams, 1975]. While the USLE uses rainfall as an indicator of erosive energy, MUSLE uses the amount of runoff to simulate erosion and sediment yield. This modification is reported to increase the prediction accuracy of the model, the need for a delivery



ratio is eliminated, and single storm estimates of sediment yields can be calculated [e.g. Wang *et al.*, 2008]. The MUSLE equation as used in SPHY is as follows:

$$Q_s = 11.8 (Q_r \cdot q_{peak} \cdot A_{cell})^{0.56} \cdot K \cdot C \cdot P \cdot LS \cdot CFRG$$

where  $Q_s$  is the sediment yield (t/d);  $Q_r$  is the surface runoff volume (mm/ha);  $q_{peak}$  is the peak runoff rate ( $m^3/s$ );  $A_{cell}$  is the area of the grid cell ( $km^2$ );  $K$  is the USLE soil erodibility factor;  $C$  is the USLE cover and management factor;  $P$  is the USLE support practice factor;  $LS$  is the USLE topographic factor; and  $CFRG$  is the coarse fragment factor.

To calculate peak runoff we use the modified rational formula [Neitsch *et al.*, 2005]:

$$q_{peak} = \frac{\alpha_{tc} \cdot Q_{surf} \cdot Area}{3.6 \cdot t_{conc}}$$

where  $q_{peak}$  is the peak runoff rate ( $m^3/s$ ),  $t_c$  is the fraction of daily rainfall that occurs during the time of concentration,  $Q_{surf}$  is the surface runoff calculated by the SPHY model,  $Area$  is the subbasin area,  $t_{conc}$  is the time of concentration for the grid cell (hr).

The fraction of daily rainfall during the time of concentration should ideally be calculated directly from sub-daily rainfall data. For this study, one station was available close to the study area with sub-daily data (see section 2.4.3). For an average time of concentration of 0.5 hr,  $t_c$  was estimated to be 50% (so half of daily rainfall falls in only half an hour).

The time of concentration is calculated using the Kerby-Kirpich method [Fang *et al.*, 2008]. This method calculates the time of concentration by adding the time of concentration for overland flow ( $t_{ov}$ ) using the Kerby method and the channel component using the Kirpich method ( $t_{ch}$ ), so  $t_c = t_{ov} + t_{ch}$ . The Kerby equation is

$$t_{ov} = 1.44 * (L * N)^{0.467} S^{-0.235}$$

where  $L$  = the overland-flow length (m),  $N$  is a dimensionless retardance coefficient and  $S$  is the slope of terrain. For the retardance coefficient, typical values agricultural areas are 0.2, and for forested areas 0.8. The Kirpich equation for channel flow time depends on channel flow length and channel slope [see Fang *et al.*, 2008].

## 2.4 Input datasets

### 2.4.1 Overview of datasets used

TNC is working on the Blueprint for the Lake Tanganyika area, and has collected several datasets required for the modelling assessment. The datasets were prepared or aggregated at a 250 m spatial resolution. In summary, the following datasets are used as input to the modeling study (more details below):

- SRTM digital elevation data resampled for erosion modeling.
- Rainfall: satellite-based FEWS dataset and rainfall station data
- Evapotranspiration: daily spatial dataset based on reanalysis data



- Soil maps: the SoilGrids dataset 250m (still in beta-version) has been processed to deliver SPHY soil input parameters.
- Land cover/change: TNC has elaborated a land cover map based on hi-res satellite imagery (Google Earth and Landsat). Also a Land Cover Change (LCC) map was made by analyzing data from different years.

These datasets and their preprocessing for the model are explained below.

#### 2.4.2 Elevation

Digital Elevation Model data are used in SPHY to derive topographic attributes of the sub-basin, including area, slope, and field slope length. SPHY uses the derived slope and flow accumulation grids as inputs to several simulation components.

The principal global DEM datasets are (i) SRTM (Shuttle Radar Topography Mission) and (ii) ASTER (Advanced Space borne Thermal Emission and Reflection Radiometer). For erosion modelling, preference is given by the scientific and modeling community to SRTM data (e.g. De Vente et al. [2009]). The DEM data from this mission cover most of the populated regions of the world and are publicly and freely available at a spatial resolution of around 30m.

From the SRTM data, the USLE topographic factor LS was calculated using the procedure described in the documentation of the hydrological model SWAT [Neitsch et al., 2005] based on slope length and slope angle.

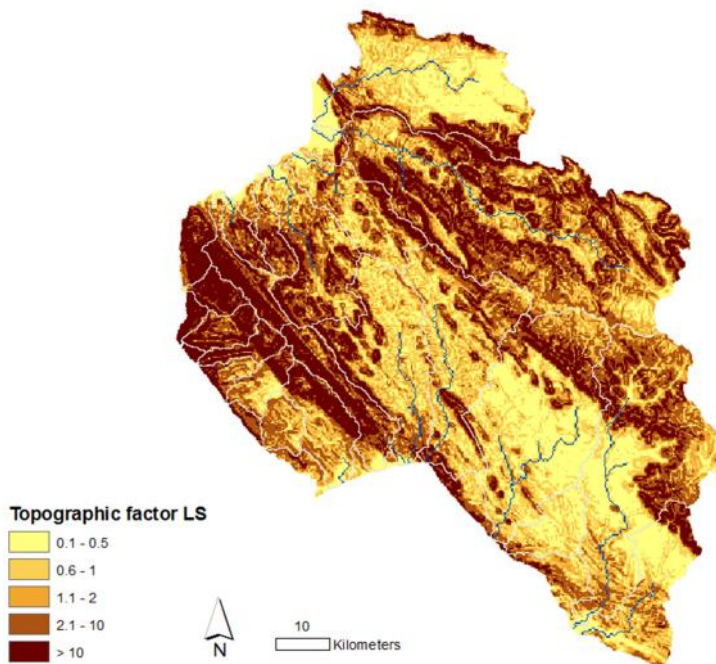


**Figure 7. Spatial distribution of the topographic USLE factor (LS)**

Based on slope, flow length and retardance factors, the SPHY model calculates the time of concentration for each cell in the area. The time of concentration determines to a large extent the peak flow and thus the amount of soil loss that becomes sediment yield entering the stream. Figure 8 shows the map of the time of concentration for the area.



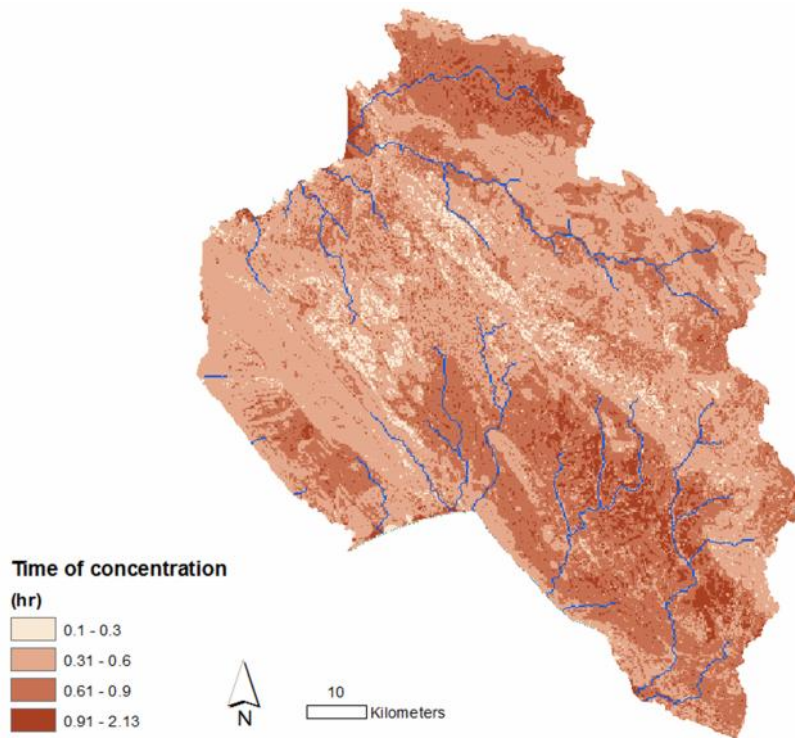


**Figure 8. Spatial distribution of the time of concentration (hr)**

### 2.4.3 Rainfall

For erosion assessments, the key input variable is rainfall: its variability (especially extremes) and spatial distribution define to a large extent the erosion patterns and sediment yields. For this study, the following data sources are available:

- A few datasets from rainfall gauges within or close to the area
- Satellite-based rainfall datasets.

**Table 1. Overview table of rainfall data**

Name	Type	Spatial resolution	Temporal resolution	Mean Annual Rainfall (MAR)	Source
Kansayana	Gauge	-	Annual	1835	www*
Myako	Gauge	-	Daily	1774	www*
Bilenge	Gauge	-	Annual	1419	www*
Kasiha	Gauge	-	Annual	1735	TNC
UPP	Gauge	-	10 min	N/A	TNC
Kigoma	Gauge	-	Daily	935	GSOD
TRMM 3b41	Satellite	25 km	Daily	1010	TNC**
FEWS	Satellite	10 km	Daily	894-1086	www.fews.net

\* non-verified sources on the internet

\*\* This dataset was obtained from a secondary source and concerns the TRMM grid cell (25x25km) covering the Mahale Mountains





**Figure 9. Locations of the rainfall gauges – in pink the border of the study area**

Table 1 shows an overview of the rainfall datasets that were available for this study and their locations in Figure 9. The Mean Annual Rainfall (MAR) in Table 1 shows significantly different values among the datasets, especially between the rainfall gauges within the area (see Figure 9) and the satellite products. The satellite products shows mean annual rainfall values of around 1000 mm in the area. The Kigoma station north of the study area shows similar values. The stations that are in the Chimpanzee reserve are the only ones for which data are available within the study area. These stations have observed higher rainfall values of 1400-1800 mm per year.

The rainfall stations within the study area are thus representative for a very specific area with abundant vegetation (evergreen forest). To verify that this area is small compared to the rest of the study area, a satellite-based vegetation greenness index (NDVI) was calculated based on multi-annual data from MODIS. Figure 10 shows the average NDVI for the study area. As can be seen, the area where the rainfall gauges are located has the highest NDVI of the entire study area. NDVI is often used as proxy for rainfall [Hunink *et al.*, 2014] so this confirms that this area receives more rainfall than the majority of the area.

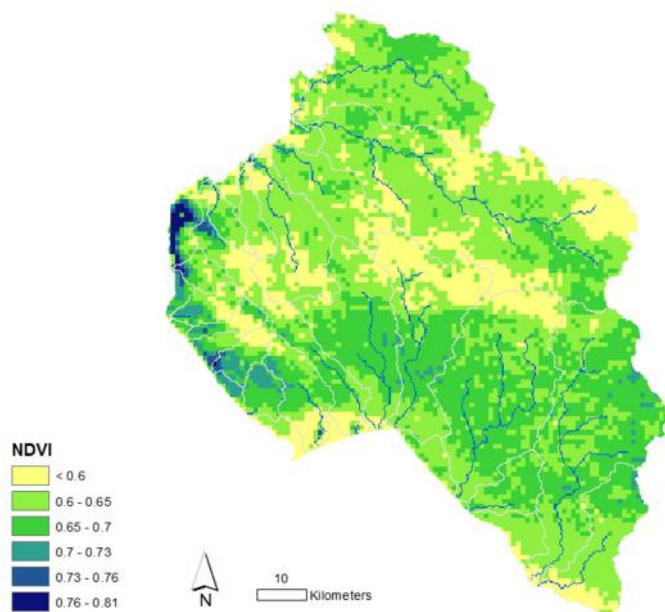


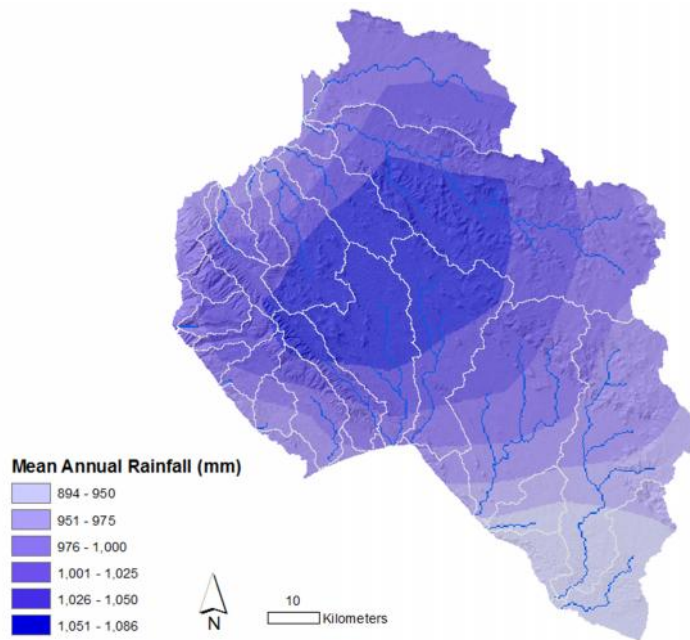
**Figure 10. Average satellite-based vegetation greenness index (NDVI from MODIS MID13A2)**

FEWS and TRMM observe similar rainfall amounts of around 1000 mm. This corresponds with the Miombo woodland (> 60% of the area) which is a vegetation type that is reported with annual rainfall amounts around 1000 mm.

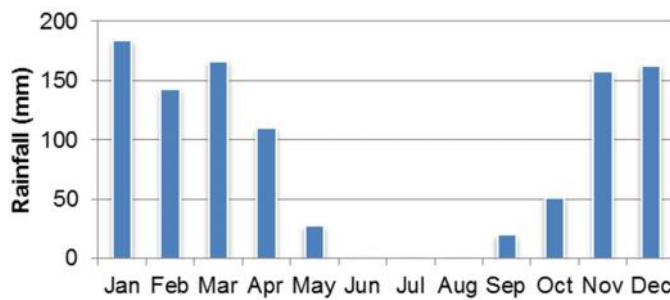
The TRMM dataset has the disadvantage of having a relatively coarse spatial resolution (25x25km). For Africa, the daily FEWS dataset (spatial resolution 10x10 km) has been successfully used for similar assessments [Droogers *et al.*, 2011; Hunink *et al.*, 2012] and was used to force the SPHY model. Figure 11 shows the Mean Annual Rainfall based on FEWS. As can be seen, the very small area with higher rainfall amounts (Figure 10) is not detected by FEWS (and neither by TRMM, not shown here). The importance of precipitation due to orographic lift of moist air from the lake requires an in-depth study on rainfall patterns in the area, but this is out of scope of this preliminary assessment.

Figure 12 shows the average monthly rainfall for the entire area based on the daily grids of the FEWS dataset.





**Figure 11. Mean annual rainfall distribution from daily FEWS data**



**Figure 12. Average monthly rainfall for entire study area from daily FEWS data**

#### 2.4.4 Evapotranspiration

To calculate potential evapotranspiration the FAO-56 method was used, based on Penman-Monteith [Allen et al., 1998]. This method multiplies a climate-dependent reference evapotranspiration rate with a crop coefficient to obtain potential evapotranspiration, or “crop evapotranspiration under standard conditions” (i.e. without stress). Thus, the potential evapotranspiration is calculated as:

$$ET_{pot} = Kc * ET_{ref}$$

Where  $ET_{pot}$  = Potential evapotranspiration [mm];  
 $Kc$  = Crop factor [-];  
 $ET_{ref}$  = Reference evapotranspiration [mm];

For the crop factor, Table 2 shows the values used for each land cover type, based on [Neitsch et al., 2005] and [Allen et al., 1998].



**Table 2. Crop factors for each land cover**

Land cover	Kc	Land cover	Kc
Rice	1.0	Evergreen forest	1.0
Bamboo	0.9	Miombo	0.8
Mixed agriculture	1.0	Residential	0.1
Palm	1.0	Herbaceous	0.9
Bare	0.5	Shrub	0.8
Wetland	1.0	Water	1.0

The daily reference evapotranspiration was calculated using the Penman-Monteith equation [Allen et al., 1998] at a 1km resolution:

$$ET_{ref} = \frac{s(R_n) + \rho c_p (e_s - e_a)}{s + \gamma(1 + \frac{r_s}{r_a})} \left( \frac{86400}{\lambda} \right)$$

Where:	$ET_{ref}$	=	Reference evapotranspiration [mm];
	$s$	=	Slope vapor pressure curve [kPa oK-1]
	$R_n$	=	Daily net radiation [W m-2]
	$r$	=	Air density [kg m-3]
	$c_p$	=	Specific heat of air = 1004 J kg-1 K-1
	$e_s$	=	Saturation vapor pressure [kPa]
	$e_a$	=	Actual vapor pressure [kPa]
	$g$	=	Psychrometric constant [kPa oK-1]
	$r_s$	=	Bulk stomatal resistance for a grass reference crop = 70 s m-1
	$r_a$	=	Aerodynamic resistance for a grass reference surface [s m-1]
	$l$	=	Latent heat of vaporization [J kg-1]

For the spatial inputs of the  $ET_{ref}$  and to calculate the daily net radiation a digital elevation map was used, daily temperature data, daily relative humidity [%]; daily mean wind speed [m s-1]; daily mean atmospheric transmissivity [-]. Most of these gridded daily variables were extracted from MERRA: a state-of-the-art NASA reanalysis dataset (<http://gmao.gsfc.nasa.gov/research/merra/>) developed for hydrological analysis on a broad range of weather and climate time scales.

The final result is a spatial dataset with daily values for reference evapotranspiration at a 1km spatial resolution. For more details on the method applied to obtain the reference evapotranspiration, please refer to [Droogers et al., 2011].

#### 2.4.5 Soil properties

A Global Soil Map of Hydraulic Properties is developed based on the Harmonized World Soil Database and uses the Van Genuchten model and Pedotransfer functions to obtain global maps at 1km (released) [Boer, 2015].

For this project, a beta-version of the 250m SoilGrids ([www.isric.org](http://www.isric.org)) dataset was used (called HiHydroSoil), obtained using the same methods as described in [Boer, 2015]. From this dataset, the following inputs for SPHY were used:

- Clay content (%)
- Silt percentage (%)



- Sand percentage (%)
- Organic Matter Content (g/kg)
- Water content between saturation point and field capacity ( $m^3/m^3$ )
- Water content between field capacity and wilting point ( $m^3/m^3$ )
- Water content between wilting point and permanent wilting point ( $m^3/m^3$ )
- Saturated Hydraulic Conductivity (mm/d)
- Coarse fragments (%)

These variables were extracted for both the root zone (taken here as 60 cm) and the sub-zone.

From the soil dataset, the MUSLE soil erodibility factor was calculated (detailed in following section) and the USLE coarse fragment factor ( $CFRG$ ), using the equation:  $CFRG = \exp(-0.053 \cdot \text{coarse})$ , where coarse is the percentage of coarse fragments in the upper soil layer (%).

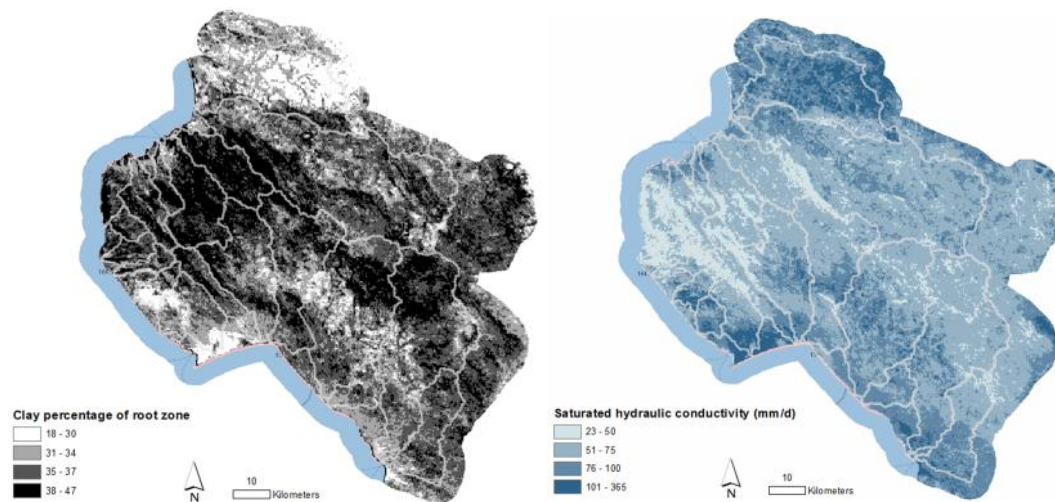


**Figure 13. Two soil parameters (left: clay percentage, right: saturated hydraulic conductivity) extracted from SoilGrids.**

#### 2.4.6 Soil erodibility

The USLE soil erodibility factor for each soil class can be calculated according to Williams [1995] which proposed the following equation:

$$K = f_{csand} \cdot f_{cl-si} \cdot f_{orgc} \cdot f_{hisand}$$

where  $f_{csand}$  is a factor that gives low soil erodibility factors for soils with high coarse-sand contents and high values for soils with little sand,  $f_{cl-si}$  is a factor that gives low soil erodibility factors for soils with high clay to silt ratios,  $f_{orgc}$  is a factor that reduces soil erodibility for soils with high organic carbon content, and  $f_{hisand}$  is a factor that reduces soil erodibility for soils with extremely high sand contents. All these factors are calculated from the fractions of each texture class as in Williams which can be found in the soil dataset used.

For the Mahale region, the K factor ranges between 0.10 and 0.15. Highest values are found in the south and northern part of the area, lowest in the western part and Mahale Mountains.

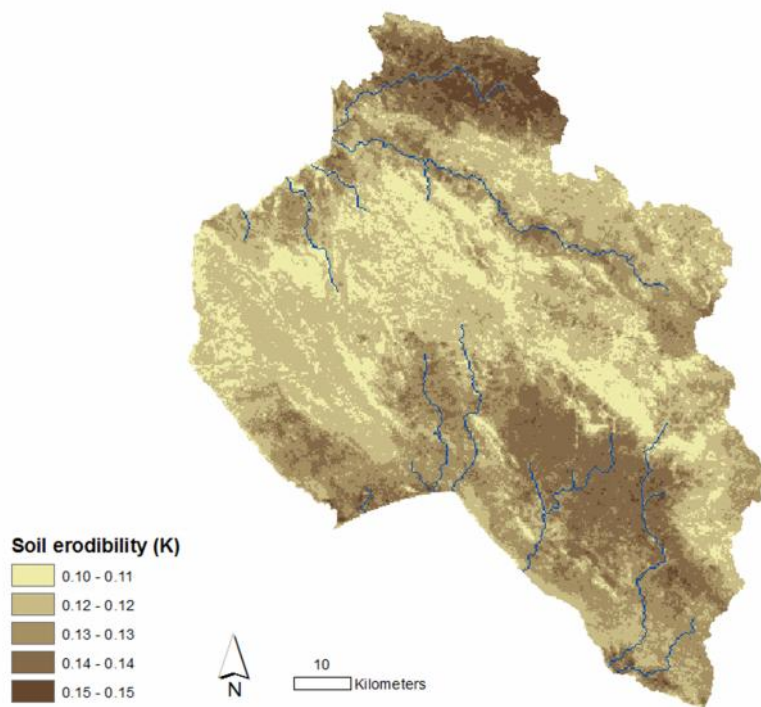


**Figure 14. Spatial distribution of the soil erodibility factor (K)**

#### 2.4.7 Land use and land cover change

TNC carried out a detailed land cover mapping assessment of the area using hi-res satellite imagery (Landsat and Google Earth-based). The map has a resolution of 30 m (Figure 15). This map was used to calculate the USLE crop management factor and the crop coefficients for evapotranspiration.

Table 3 shows for each of the land use classes the percentage area of the total area of the watershed. As can be seen, Miombo woodland is the main crop type, covering more than 60% of the area. Bamboo is principally found at the western slopes of the Mahale mountain range. Palm, Rice Wetland and Shrub cover a very small part of the total area, and are located in the downstream coastal areas. Herbaceous cover is found in the higher parts of the mountainous areas. Agriculture is principally found near the coast and in the valley bottoms and riverine areas.



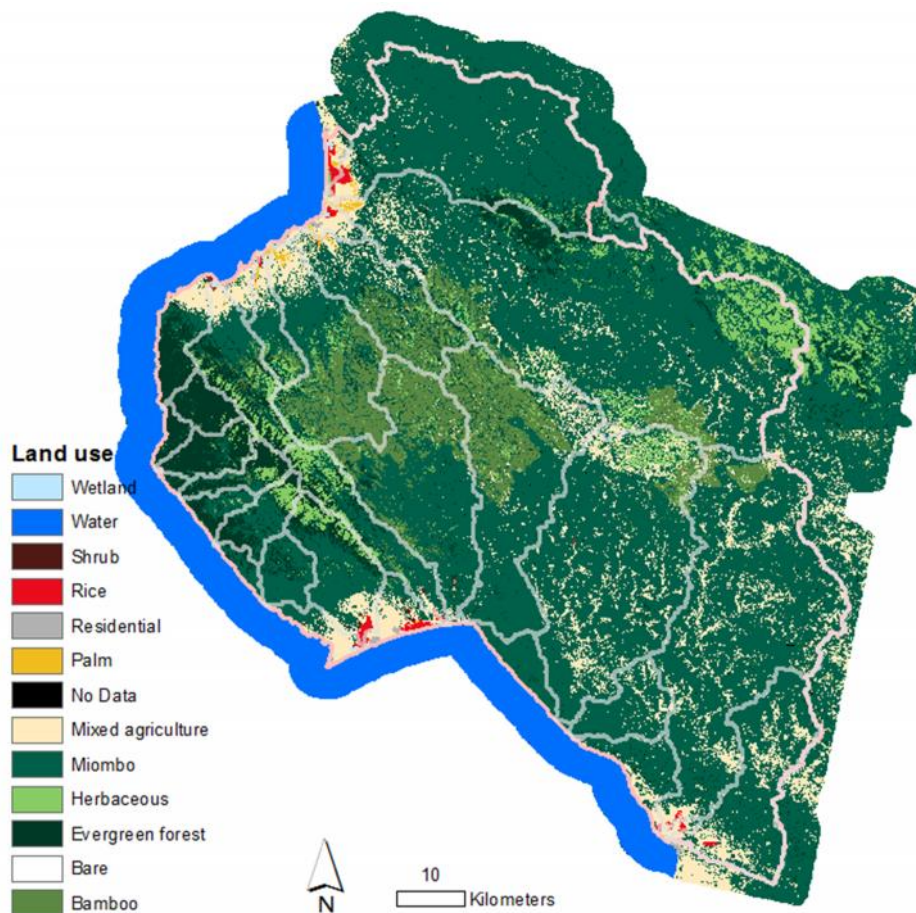


**Figure 15.** Land use map for the study area. The modeling domain corresponds to the area delimited with the pink line.

**Table 3.** Total area and relative share of each land use class based on map in Figure 15.

Land use	Area (km <sup>2</sup> )	Fraction of total (%)
Rice	29	0.3
Bamboo	663	7.0
Mixed agriculture	866	9.2
Palm	18	0.2
Bare	6	0.1
Wetland	4	0.0
Water	923	9.8
Evergreen forest	623	6.6
Miombo	5826	61.6
Residential	16	0.2
Herbaceous	474	5.0
Shrub	6	0.1
<b>Total</b>	<b>9455</b>	<b>100</b>

The mixed agriculture class corresponds to a mixture of crops, mainly cassava and maize, but also vegetables. Table 3 shows a outcomes of a socio-economic survey carried out in 2011 in the area.



**Table 4. Crops cultivated by farmers according to the socio-economic survey in 2011 in the area (source: TNC)**

Crops	Total
Cassava	48%
Maize	45%
Vegetables	8%

In spite of the reported abandonment of slash-and-burn agriculture [Itoh *et al.*, 2012], still considerable land conversion to agriculture is taking place in the area. TNC elaborated a map of land conversion based on Landsat imagery analysis over a period of 10 years. The map shows that more than 500 km<sup>2</sup> were converted to agriculture over this period. About half of these areas are located in the downstream coastal areas, and the other half in the upstream areas in the areas next to rivers with little slope. Agriculture in the riparian zone can influence the erosion hazard to a large extent: it may either function as a buffer but may also be a source of erosion depending on agricultural practices, distance from river, and other factors.

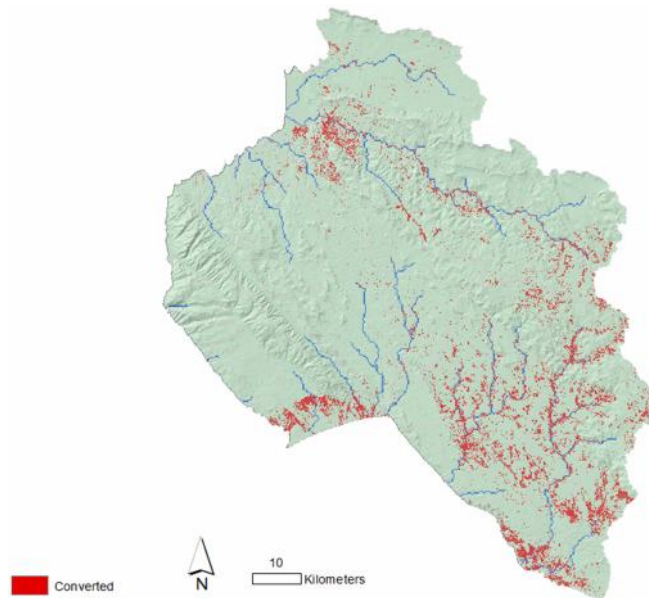


**Figure 16. Land conversion to agriculture (source: TNC)**

Agriculture in the riverine zone can have a negative impact on vegetative protection for bank erosion as vegetation influences the critical shear stress. We assume that recently converted agriculture in the riverine has lowered the channel protection by a factor 3 which is comparable to conversion from sparse trees to grassy [Julian and Torres, 2006; Arnold *et al.*, 2013]. Follow-up field surveys could study whether indeed river bank protection has reduced and how in riparian areas that were recently converted, and thus verify this assumption.

#### 2.4.8 Wildfire

An important factor for erosion in the Mahale region is wildfire. Wildfires are set outside the Park by hunters and farmers in the dry season, and frequently burn out of control, causing a major amount of damage to undisturbed habitats both within and outside the National Park. The high fire frequency in some areas does not allow forest and woodland to regenerate, causing



reduced soil cover and protection for erosion. Grasslands are likely to recover more quickly than bushlands after a fire [Pelkey, 2000].

Increasing fire frequency reduces the growth of the small plants covering the soil surface in the woodlands, and will therefore increase the erosion hazard. A satellite product was used from the MODIS platform, prepared and elaborated by TNC to a map showing the spatial distribution of number of annual events. The MODIS algorithm detects the approximate date of burning (at 500 m resolutions) by locating the occurrence of rapid changes in daily surface reflectance time series data [Boschetti et al., 2009]. From this date, a fire frequency map for both the dry season and the wet season was produced by TNC.

For fire frequency analysis, both the dry season and wet season fires were used to calculate the fire return interval (Figure 17). Dry season fires cause reduced soil cover from which vegetation is likely to recover very slowly, thus contributing to the erosion hazard during less frequent rainfall events in or just after the dry period. Fires in the wet season may cause more immediate erosion due to imminent rainfall.

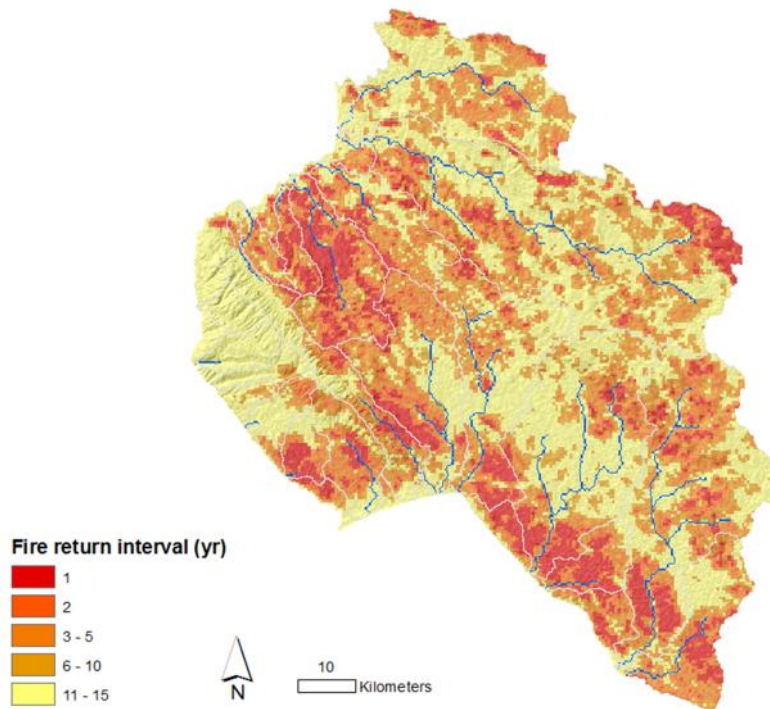


**Figure 17. Fire return interval for the study area**

Fire frequency is related to biomass and soil cover: in areas where fires are more frequent, soil and residue cover is reduced. To the best of our knowledge, no studies exist that establish direct empirical relationships between fire frequency and soil cover for this type of ecosystem. However, specifically for Miombo woodland (the major land cover in this area), one particular study [Ryan and Williams, 2011] has analysed fire frequency and its impact on biomass for a similar area in Zimbabwe. Ryan and Williams [2011] have established relationships between fire return interval and aboveground stem carbon stock for this ecosystem type. They found a more or less linear relationship for medium intense fires with fire return intervals between 1 and 10 years. For this study we assumed that this linear relationship applies also to soil cover and used this for the calculation of the crop management factor.



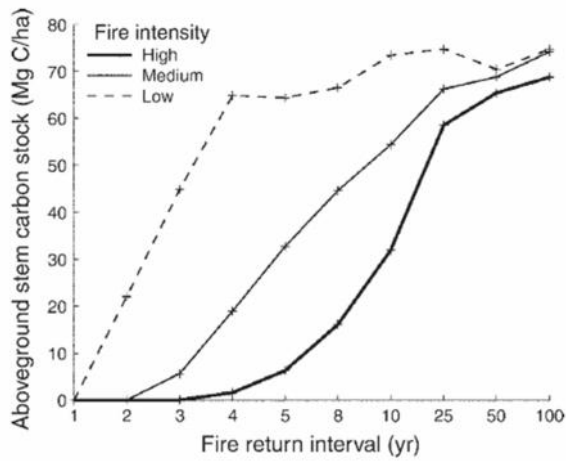


**Figure 18. Aboveground tree carbon stock against fire return interval for three fire intensity classes (source [Ryan and Williams, 2011])**

#### 2.4.9 Crop management and practices

The crop management factor of the USLE equation ( $C$ ) is defined as the ratio of soil loss from land cropped under specified conditions to the corresponding loss from clean-tilled, continuous fallow [Wischmeier and Smith, 1978]. The crop management factor was calculated using the following equation [Neitsch et al., 2005]:

$$USLE_C = 0.8^k + USLE_{C0}^{(1-k)}$$

$$k = \exp(-0.00115 * SOL_{COV})$$

where  $USLE_{C0}$  is the original minimum of the USLE cover factor and  $SOL_{COV}$  is the soil cover residue (kg/ha).  $USLE_{C0}$  was obtained from standard values used in the SWAT model [Neitsch et al., 2005]. This value depends on land cover, and ranges between 0.0001 (evergreen forest) and 0.2 (Mixed agriculture).  $SOL_{COV}$  was derived using the linear relationship found by Ryan and Williams [2011], assuming wildfires with low intensity are dominant and a conversion rate from aboveground carbon stock to residue of 2%.

The above results in the spatial distribution of  $USLE_C$  as represented in Figure 19. Relative high values are found for agricultural areas upstream and near the coast and for the frequently burned areas in bamboo and Miombo woodland zone.



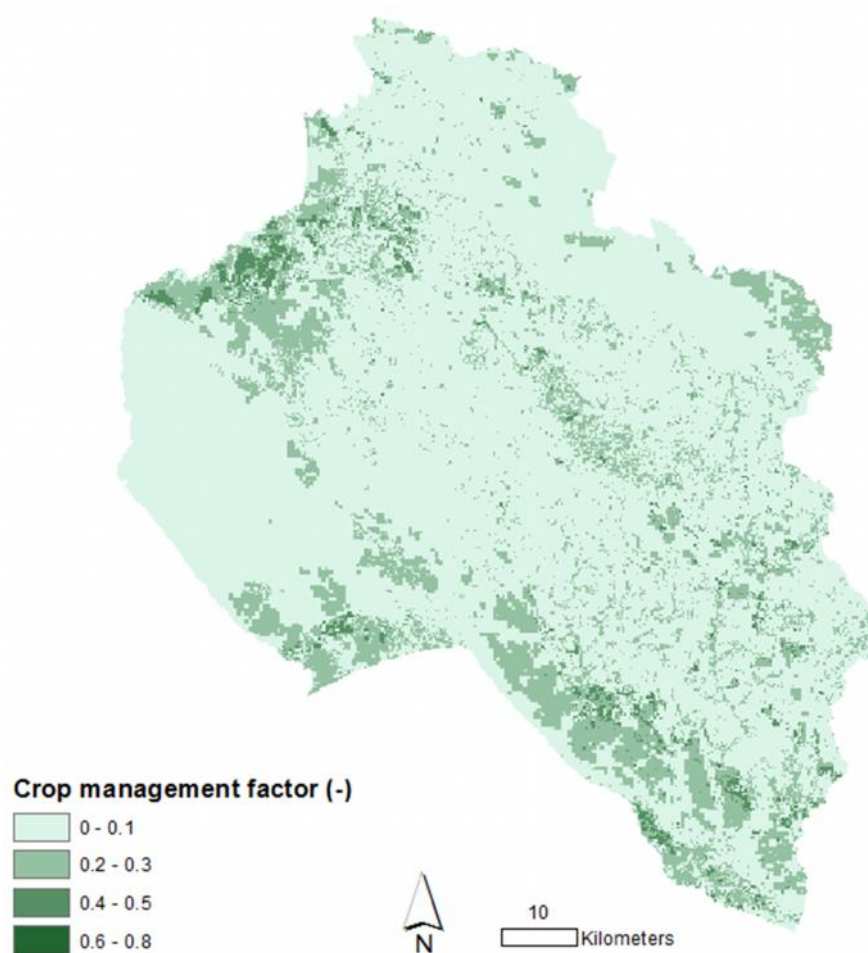


**Figure 19. Spatial distribution of USLE crop management factor**

No reliable data are currently available on farmers' practices to derive the MUSLE support practice factor (P). Therefore the following was assumed:

- Agricultural land > 10years: P = 0.75 (typical value for cross slope farming)
- Agricultural land converted during the last 10 years: P = 1.0 (typical value for up and down slope farming)

This summarizes that farmers who have recently started to cultivate new lands are less likely to have developed sustainable land management practices.

## 3 Results

The SPHY model was run with a daily timestep over a 10-year period at a spatial resolution of 250x250 meter. Daily outputs were also summarized to monthly and annual values, and time series were extracted for the principal catchments in the area.

The sections below summarize:

1. Spatial patterns of runoff and erosion
2. Sediment yields of the catchments
3. Relationship with land use and management
4. Preliminary priority areas

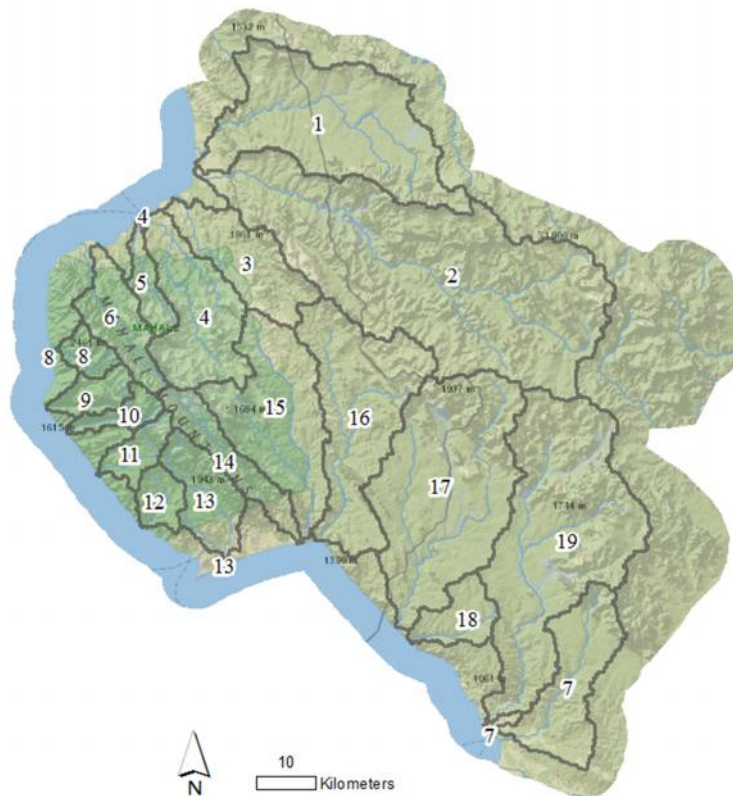


**Figure 20. Principal catchments in the study area**

### 3.1 Spatial analysis of runoff and erosion

Figure 21 shows the mean annual runoff and mean annual erosion for the study area. As expected, patterns of runoff and erosion are linked: many areas with high runoff have also high erosion rates. However, in those areas with high runoff and steep slopes combined with dense vegetation substantially lower erosion rates occur.. This is especially the case for the western slopes of the Mahale mountains (catchments 8-11), where runoff is relatively high due to the steep slopes and rainfall amounts, but erosion is relatively low due to the protection of soil by the evergreen forest on this side of the mountain range. The eastern slopes of the Mahale mountain range (catchments 4 and 15) are relatively prone to erosion due to wildfires and lower vegetation cover (see also section 3.2).



For the northern and southern parts of the study area, runoff and erosion is relatively low: these basins have a relatively low slope, and especially catchment 1 (see Figure 20) has hardly any cultivated areas.

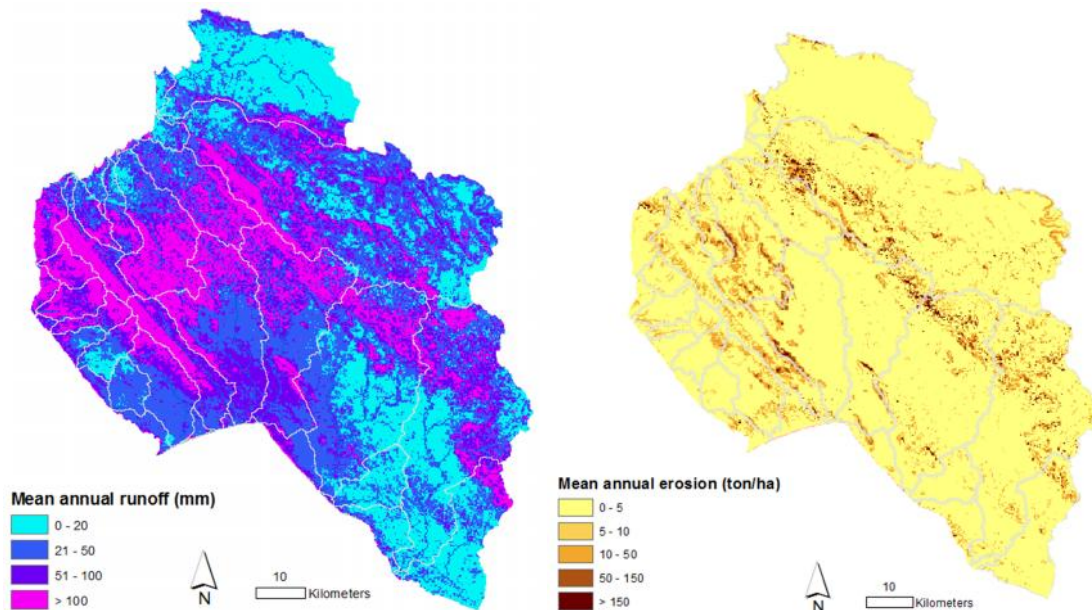


**Figure 21. Mean annual runoff (left) and mean annual erosion rate (right).**

Figure 22 provides insight in the processes that influence runoff rates. These scatterplots are based on each simulation cell (more than 10,000) and show in the lower part the relationship between mean annual runoff (y-axis) based on the daily simulations, and 4 model input variables (x-axis):

- The saturated hydraulic conductivity – determining to a large extent the infiltration capacity
- Slope
- Elevation
- Mean annual rainfall (mm)

In the upper part of Figure 22 (reddish) the histogram of those four variables is shown as well.

As can be seen (from left to right in Figure 22):

- Runoff is lower where infiltration capacity is high. For high values of saturated hydraulic conductivity there is no significant influence anymore
- There is a relationship with slope, as expected. The highest runoff rates are found in residential areas.
- The highest runoff rates are in the lower areas, and medium elevations. The higher elevations are well protected and have lower runoff.
- A clear relationship with mean annual rainfall, as can be expected: high rainfall leads to high runoff.

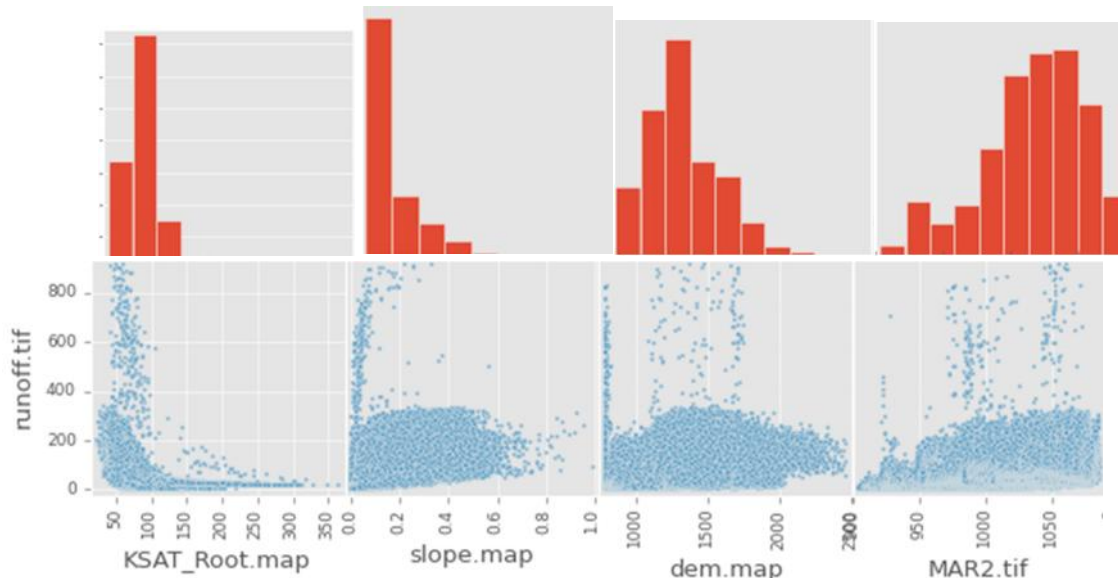


**Figure 22. Annual runoff (mm) against (i) saturated hydraulic conductivity (mm/day), (ii) slope (m/m), (iii) elevation (masl), and (iv) mean annual rainfall (mm/y). Histograms of the area of the four variables on the x-axis are indicated as well (top).**

Figure 23 shows the erosion for the driest year in the analysis period (2003) and the wettest year (2009). These outputs highlight the importance of rainfall as a driver of erosion. In the dry year, erosion rates of above 50 tons/ha are concentrated in the higher steep parts with agricultural use, Miombo woodlands or bamboo. For the wet year, these rates can be found mainly in the same land use types, but covering larger areas across the region.

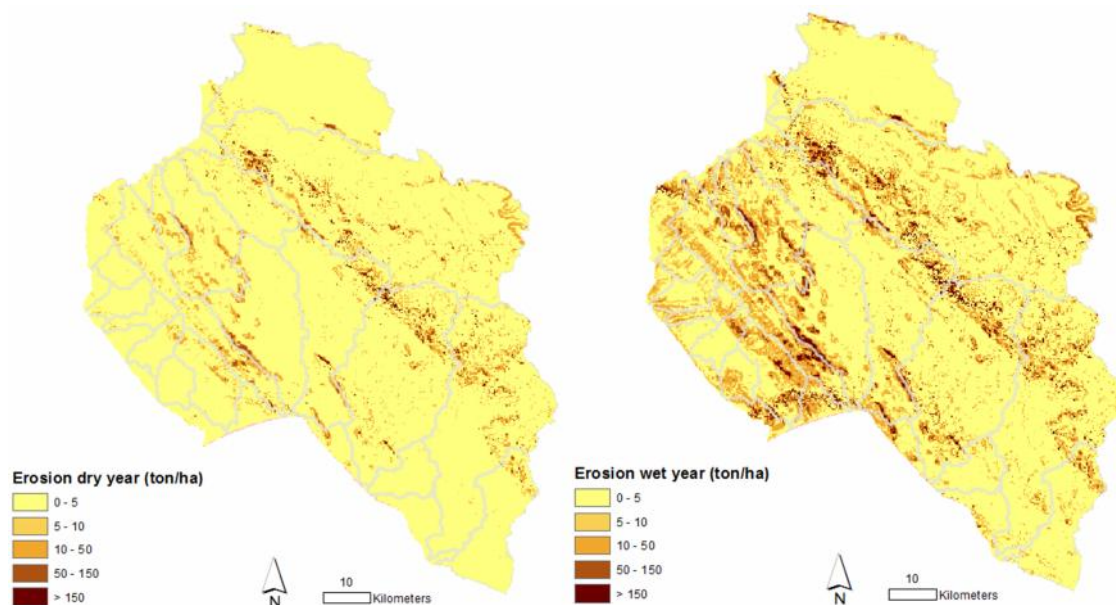


**Figure 23. Annual erosion during a relatively dry year (2003, left) and a wet year (2009, right).**

### 3.2 Land use and management

There is a clear relationship between land use and land use management and erosion rates. Table 5 and Figure 24 show mean annual sediment yield per land use class and the specific



sediment yield (tons/ha). In the table, also average fire return interval average slope and average drainage area for each land use class is shown.

**Table 5. For all land use types: total area, total annual sediment yield, specific sediment yield, average fire return interval, average slope and drainage area**

Land use class	Area (km <sup>2</sup> )	Total yield (tons/yr)	Specific yield (ton/ha/yr)	Fire return interval (yr)	Average slope (m/m)	Average drainage area (km <sup>2</sup> )
Bamboo	652	798,374	12	3	0.10	2
Bare	4	15,631	36	6	0.08	1
Evergreen forest	571	117,894	2	8	0.22	6
Herbaceous	354	224,023	6	3	0.15	1
Miombo	4,509	1,248,144	3	4	0.09	6
Agric. (non-conv)	471	1,534,464	33	4	0.06	16
Agric. (converted)	255	652,180	26	4	0.04	27
Palm	17	30	0	10	0.01	71
Residential	14	3,746	3	11	0.04	0
Rice	31	352	0	13	0.01	57
Shrub	6	288	0	7	0.04	27
Water	21	0	0	0	0.00	0
Wetland	4	2	0	15	0.00	10

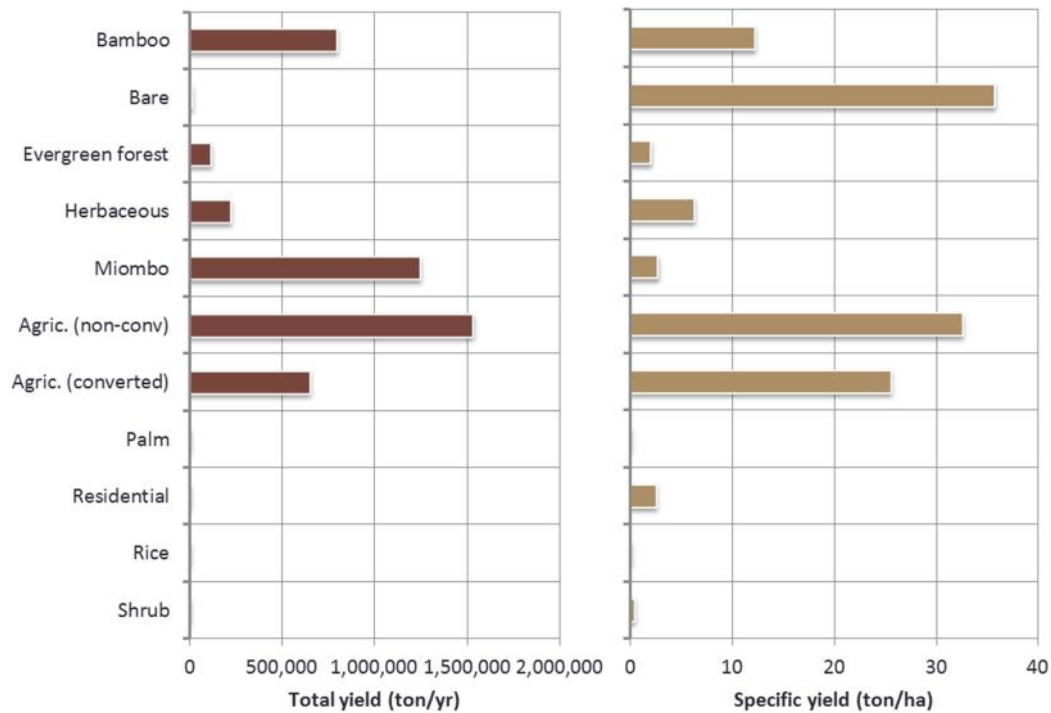


**Figure 24. Specific yield (ton/ha) and total sediment yield per land use class, based on 10-year average.**

Based on these results the following conclusions can be drawn:



- **Bamboo:** The bamboo zone is a fire-prone area (average fire return interval is 3 years but in many places annual wildfires take place) and has relatively steep slopes. This leads to low protective vegetative cover and high runoff rates. Bamboo however is a fast-growing grass that recovers relatively fast. Still, this area contributes around 17% of the total sediment load in the area.
- **Bare:** Bare areas are often found close to agricultural areas, suggesting they may be abandoned agricultural areas in a degraded state. They may as well be just bare rock areas, and thus not contributing to sediment loading. In this study, it was assumed that half of the bare areas are contributing (with soil), half not (no soil). Specific yield of this type of areas is high, stressing the need to promote land conservation and mitigate degradation. There is little area classified as “bare” in the study area, so the total contribution to erosion is low.
- **Evergreen forest:** In spite of being located on very steep slopes, this land use type contributes relatively little to the total erosion hazard as it provides good vegetative cover to the soil and does not experiencing wildfires.
- **Herbaceous:** These lands are fire prone and although grasslands generally provide good protective cover against erosion, the fire hazard causes soils to be uncovered during part of the year and thus increases the erosion hazard.
- **Miombo woodland:** Miombo is by far the principal land cover (>60%) in the region, and contributes considerably to the erosion hazard (27%). Fires are common in some parts of the area for this type of woodland. Also some areas are relatively steep.
- **Agriculture:** see below
- **Other:** Palm, Rice, Shrub and Wetland are all land covers that are located in the downstream areas, with gentle slopes with no or hardly wildfires, providing good protective cover.

Comparing the obtained erosion rates for agriculture with typical values for this part of Africa [Cohen *et al.*, 2006], we observe that the croplands are in the higher range of what is commonly observed (between 30-45 tons/ha). So are grasslands and bamboo, due to the impacts of wildfire.

### Agriculture

Many of the agricultural areas have been converted only recently to cultivation. The assessment by TNC of land conversion based on Landsat imagery allows obtaining some insight in potential impacts on sediment production of this process. Table 5 specifies between agriculture that was recently cultivated and the areas that are under cultivation during longer time (> 10 years).

The agricultural area has increased by more than 50% over the last 10 years. Generally these new areas are located in the downstream parts of the catchments (drainage area on average around 70% bigger), and in the riparian zones. Most of these areas have very gentle slopes (on average 3.8% for the newly converted areas compared to 6.4%) and are more suitable for cultivation. The analysis shows that the newly cultivated areas contribute an additional 14% of sediment to the total sediment yield of the area.

In the riparian areas, bank erosion can be a significant additional source of sediment, due to a reduction in the vegetative cover of the riverine zone. For this study, no data were available on the potential impact of bank erosion, very dependent on river morphology. Future surveys can provide more insight in the relative importance of this sediment source.



## Wildfire

The impact of fire on the erosion hazard is presented in Figure 25. Here, fire return interval (on average how many years between wildfire events) is plotted against the average erosion rate in tons/ha. Bamboo, being the principal fire-prone area, shows the highest dependency with fire return interval. The analysis indicates erosion rates of above 30 tons/ha for bamboo areas that burn yearly, while the erosion hazard is reduced significantly for areas where fires are less frequent. The analysis assumes that soils in these areas are not depleted as vegetation recovers quickly after burning.

Herbaceous areas (in the higher elevations) and the Miombo woodland show a similar relationship. Erosion rates of around 10 tons/ha are predicted for areas that burn yearly.

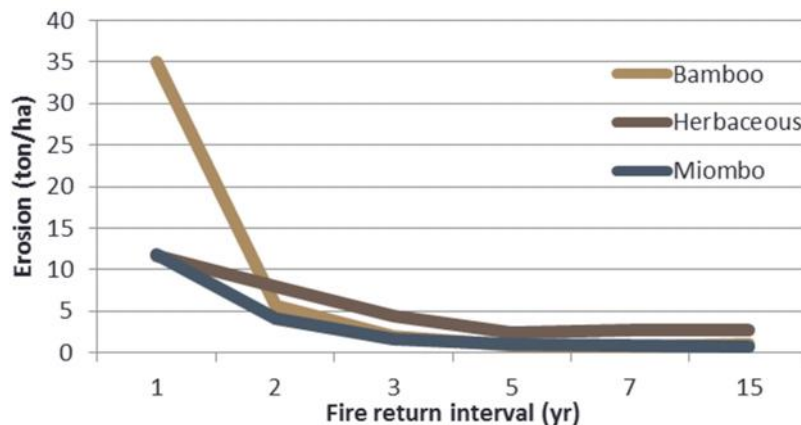


Figure 25. Fire return interval and erosion for three land use classes affected by wildfires

### 3.3 Sediment yield into Lake Tanganyika

The hydrological flow regime is critical for the transport capacity and the type of sediments that are transported. The sediment grain size composition determines to a large extent the impacts on the lake ecosystem. Fine-grained materials are able to travel further into the lake, but at the same time, coarsely grained and low-organic particles can have more severe local impacts [Eggermont and Verschuren, 2003].

For this study, no monitored streamflow data are available, but the hydrological model can be used to obtain insight in the flow regime, and its partitioning in direct runoff, lateral flow and baseflow. Baseflow is reported to be a significant component in the tributaries of the Lake Tanganyika basin, and support the transport of fine clayey materials [West, 2001].

Figure 26 shows the monthly flow regime (based on averages over the 10-year simulation period) for four catchments of different size (see Figure 20) in the area. As can be seen, surface runoff is the main component in the start of the rainy season, while baseflow becomes more important when the dry season approaches. Minimum flows in the dry season are around 1 m<sup>3</sup>/s, depending on the catchment characteristics. The largest catchment (2) reaches maximum flows of around 30 m<sup>3</sup>/s in the wet season. For the entire area, the baseflow component corresponds to about 65% of the flow, and runoff (direct and lateral) for about 35%.



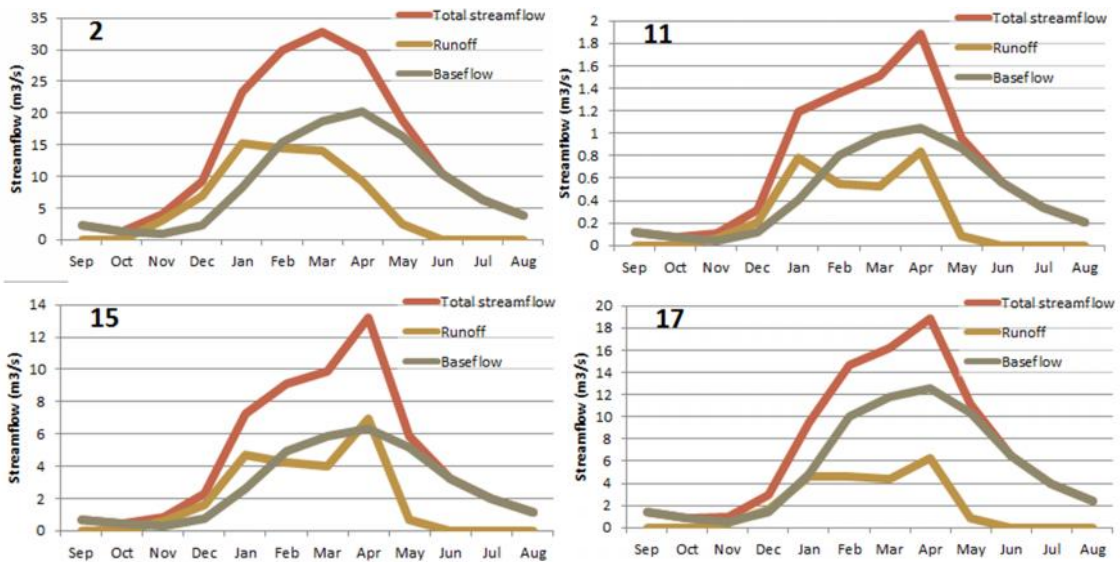


**Figure 26. Monthly runoff and baseflow regime for 4 selected catchments in the area, starting in middle of dry season**

From the SPHY model, total sediment yield entering streams can be extracted for each point of interest. Figure 27 shows mean annual sediment yield entering the lake for each of the catchments. The size of the dots indicates the relative contribution to the total sediment input of the area. Total sediment contribution per catchment ranges between 5,000 tons/year to around 1 million tons/year.

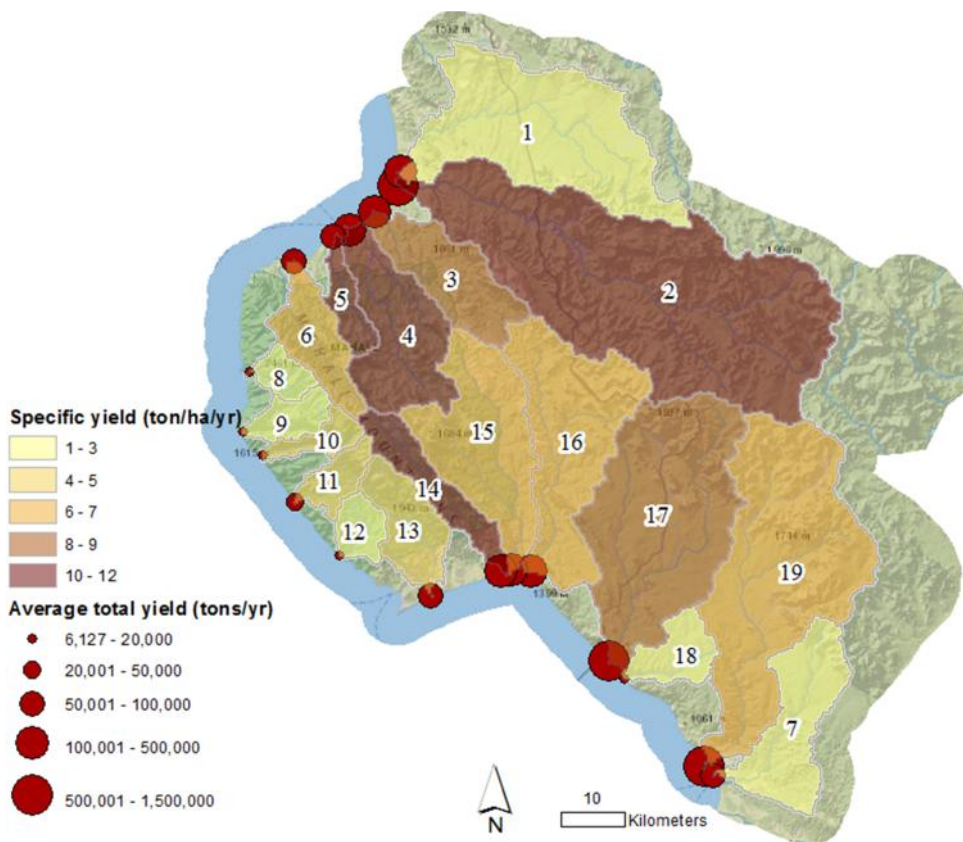


**Figure 27. Mean annual sediment yield (tons/yr) and specific yield (total yield divided by area) for each catchment in the area**



Figure 27 shows the specific sediment yield which is calculated as the mean annual yield divided by the area of the watershed. This indicates which of the watersheds are most suitable for potential interventions.

Table 6 shows partly the same information as Figure 27, including model estimates of the maximum annual sediment yield corresponding to the wettest year 2009 of the simulation period. As can be seen, during wet years, sediment yields at the catchment level can be at least twice as high as on average. This highlights the importance of rainfall as the principal driver of erosion, and the need to capture well its temporal and spatial variability. Also, dynamic approaches like used in this study are preferable for this reason to estimate erosion levels.

The estimates given in this table are based on field-level sediment yield. The model does not simulate sediment dynamics in the channels. In other words, it assumes a sediment delivery ratio of 1 (so all sediment load entering the stream on the long-term reaches outlet of watershed). This is reasonable at the longer term, especially for the smaller catchments.

For larger watersheds, sediment produced in upper basins does not immediately flush out to lower basins, but can be deposited in the riverbed. Subsequently, large flood events flush these sediments periodically downstream. For example, extreme rainfall events in 1961-62 have been linked in the study area with sediment accumulated in the lake [Cohen *et al.*, 2005].

**Table 6. Mean annual yield and maximum annual yield (year 2009), total and area-specific for each watershed**

Water-shed	Area (km <sup>2</sup> )	Mean annual yield (tons/yr)	Mean annual specific yield (ton/ha/yr)	Max annual yield (tons/yr)	Max annual specific yield (ton/ha/yr)
1	650	166,055	3	279,542	4
2	1379	1,376,339	10	2,300,203	17
3	241	198,317	8	347,624	14
4	316	345,359	11	657,730	21
5	72	83,897	12	170,742	24
6	160	98,566	6	188,327	12
7	282	82,690	3	109,757	4
8	55	16,170	3	31,557	6
9	74	18,202	2	38,214	5
10	59	19,396	3	47,429	8
11	75	23,917	3	80,897	11
12	68	7,331	1	49,249	7
13	163	74,964	5	381,280	23
14	145	150,473	10	564,982	39
15	423	257,160	6	717,543	17
16	501	336,478	7	800,384	16
17	739	559,993	8	1,003,769	14
18	107	6,127	1	16,268	2
19	837	575,418	7	690,862	8



The model simulations provide daily outputs and provide insight in how extreme events relate to total and mean values. Like everywhere, most erosion occurs in a few events. Peak sediment input enters the stream, and then depending on the hydrological flow regime, finds its way to the watershed outlet.

To better understand how daily extremes relate to the annual pattern, Figure 28 shows the daily sediment yield for 4 selected watersheds (see ID in the figure), for a dry (2003) and a wet (2009) year. It shows that most sediment is produced during the wet season during a few peak events. Runoff rates and transport capacity are highest during these events. Depending on the size of the watershed and channel dynamics these peaks can be attenuated to some level.

Especially in the middle of the wet season, when soils are saturated and runoff peaks, sediment yields are high. In volumetric sense, the model indicates that sediment yield is very low during dry season. Still, low flows during the dry season may carry finer material that could be relevant for impacts on the lake's fish habitats. More data are needed to better understand flow regime and its relation to sediment transport capacity and grain size.

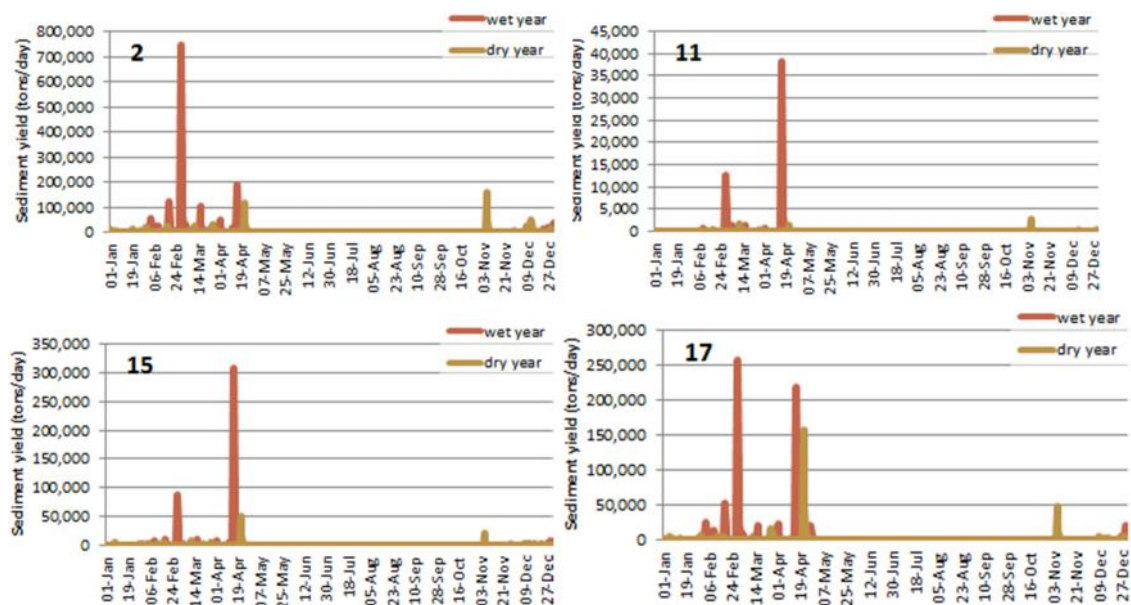


**Figure 28. Daily sediment yield (tons/day) for a dry year (2003) and a wet year (2009) for 4 selected catchments in the area**

### 3.4 Preliminary selection of priority areas

A preliminary selection of target areas was carried out based on the following assumptions:

1. Areas where erosion is above 5 tons/ha are potentially good places for the promotion of sustainable land management practices (terracing, etc)
2. Bamboo zone and miombo woodland where annual fires take place should be targeted as they have a relatively high contribution to total sediment yield.
3. Areas with gentle slopes and not (yet) used for agriculture are susceptible to land conversion by local communities. Areas targeted are those where slope is below 10% and no agricultural activity is taking place.





**Figure 29. Preliminary map of priority areas based on the erosion modeling assessment**

Figure 29 shows the map with the targeted areas based on these three criteria. Sustainable land management practices focus on the lower areas close to the lake, and agriculture on higher areas with steep slopes, and riparian areas.

For intervening in the agricultural areas, the promotion of soil and water conservation measures should be considered. These measures have been studied in many parts of the world, including in Tanzania and areas with similar biophysical conditions. A large database with qualitative estimates on the agricultural and downstream benefits of sustainable land management measures is the WOCAT database [WOCAT, 2007].

Sustainable land management technologies that could potentially reduce the erosion hazard in this region are (but not limited to):

- Bench terracing and similar technologies, to reduce the effective slope of agricultural lands
- Protection of riverine areas by planting adequate species and control
- Promote alternatives to charcoal production (e.g. fuel-efficient stoves)

- Agroforestry activities in Miombo woodlands that are at risk of being converted to agriculture [*Sileshi et al.*, 2007]
- Reforestation in upstream degraded areas with adequate species, considering possible impacts on hydrological regime



**Figure 30. Examples of sustainable land management technologies (left: bench terracing, right: riverine protection). Source: WOCAT database**

For several of these measures the potential impact of these measures can be quantified by means of pilot and demonstration projects, and/or modeling assessments [e.g. *Hunink and Droogers*, 2015].



### 4.1 Main findings and recommendations

This report summarizes the erosion modeling assessment of several pilot watersheds in the Greater Mahale Ecosystem, part of the Lake Tanganyika basin. The hydrological model SPHY was applied using the sediment module based on the MUSLE approach, to assess hydrological flows, erosion and sediment yield on a high spatial and temporal resolution. Results show the spatial and temporal variability of erosion and a better understanding of relationships with land use and management. Additionally, a preliminary assessment of priority areas for conservation activities was carried out.

The analysis shows that there are several key factors that contribute to the spatial and temporal variability of erosion that should be taken into account for erosion mitigation and soil conservation measures. The principal factors that were identified are:

- *Rainfall*: Erosion and sediment yields are directly related to rainfall amounts and its spatial variability which is high in this area. This highlights the need for better understanding rainfall patterns in the area, and the possible impact of changes in rainfall dynamics because of climate change on the erosion hazard.
- *Slope*: The sediment yield from areas that were recently converted to agriculture depends to a large extent on the slopes of newly cultivated lands.
- *Runoff*: Runoff drives erosion especially on the steep slopes of the mountain ranges with high runoff. Erosion hazard can be reduced significantly where good protective vegetation covers is present such as the evergreen forest in the Mahale Mountains.
- *Baseflow*: The analysis shows that at least more than half of streamflow is originating from baseflow. These flows tend to transport finer material (clayey), potentially also in the dry season, and may be critical for understanding better the impacts on the lake ecosystem.
- *Fire*: Areas in the Miombo woodland and bamboo zone where frequent fires occur (each 1-3 years) are likely to have less biomass to protect soils. The analysis shows that this is a key factor for erosion mitigation in this area.
- *Bare / degraded*: Although only very small parts of the area were classified as bare, they may be a considerable source of erosion if agricultural lands lose their production potential and convert into degraded lands.

Key areas that are identified for potential intervention and protection are those where: (i) wildfires take place often and cause significant sediment loads, (ii) areas that are currently cultivated and where erosion is relatively high, and (iii) areas with gentle slopes where no agricultural activity takes place, but having a high likelihood of being converted in the near future.

Given the relatively high contribution of agricultural lands and fire-prone areas, this study concludes that there is a high potential for reducing the erosion hazard and therefore having a positive impact on the fish habitat in the lake and the livelihood of the coastal communities.



## 4.2 Potential future analysis steps

Potential future analysis steps are summarized here that can support the efforts of TNC and its partners to understand links between the environment and livelihoods. This will lead to enhancing the protection of the Mahale Greater Ecosystem and the Lake Tanganyika basin by supporting livelihoods of local communities.

### Rainfall

Very high gradients in rainfall regime were detected in this scoping study. The high elevations of the mountain ranges cause moist air from the lake to lift, producing locally high rainfall amounts. Vegetation types and patchy data on climate in the area indicate that other areas receive considerably less rainfall.

Available ground-data are not sufficient to capture rainfall patterns in the area. No long-term records are available on representative locations. Global datasets are used as an alternative in this study. On the one hand, several climate datasets are available that do capture the spatial variability, but are not fit for hydrological modeling as they concern only long-term averages. On the other hand, an increasing number of remote sensing-based rainfall products are available that have shown to perform well for dynamic hydrological modeling. However these datasets have a low spatial resolution.

By combining both types of datasets, a more accurate rainfall dataset can be obtained that captures both the temporal as the spatial variability. Different methods are currently available to generate such high-resolution rainfall datasets for specific areas of interest and are relatively straightforward to apply [e.g. *Hunink et al.*, 2014].

### Upscaling and data

The current analysis can be considered as a “proof of concept”. Outputs have been shown to be sound and consistent with the few data available on the area and data from similar areas. With relatively little effort, this modeling approach can be scaled to other parts or the entire Lake Tanganyika basin.

To improve the accuracy of the modeling approach, more field data can be gathered the sediment *source* and *sink* (i.e. Lake), by:

- *Source*: Measuring sediment loads in streams require long-term measurement campaigns that are costly. As an alternative, field surveys can be carried out that consists of a survey based on visual interpretation of erosion features, using a semi-quantitative scoring methodology [*de Vente and Poesen*, 2005; *de Vente et al.*, 2006]
- *Sink*: Studying lake bathymetry and analyzing sediment cores allows a multi-annual overview of past sedimentation rates (last decades) but in principle less useful for understanding current conditions.

### Climate change impacts

Climate change is likely to impact the Lake Tanganyika considerably [*O’Reilly et al.*, 2003] and its basin hydrology (Seimon 2015). Changes in the water balance can affect natural vegetation and animal habitats, crop production, erosion and the lake dynamics.

The model SPHY has been used often for climate change impact assessments [*Immerzeel et al.*, 2010; *Lutz et al.*, 2014]. Commonly, a baseline model is compared with simulations using



modified future climate inputs. The baseline model built for the current study can be used for understanding climate change impacts on:

- Streamflow regime
- Erosion and lake sediment inputs.
- Water stress of natural vegetation
- Water stress of agricultural areas

Climate modeling activities currently going on for the Lake Tanganyika region (such as the CESM Team, Appalachian State University and NCAR, USA) can potentially be used as input for such a climate impact assessment study, either previously downscaled or not. Other issues, such as impact on crop growth and water quality, could be relevant as well.



## 6 References

- Allen, R. G., L. S. Pereira, D. Raes, and M. Smith (1998), Crop evapotranspiration - Guidelines for computing crop water requirements,
- Arnold, J. G., J. R. Kiniry, R. Srinivasan, J. R. Williams, E. B. Haney, and S. L. Neitsch (2013), *SWAT 2012 Input/Output Documentation*.
- Van Bocxlaer, B., R. Schultheiß, P.-D. Plisnier, and C. Albrecht (2012), Does the decline of gastropods in deep water herald ecosystem change in Lakes Malawi and Tanganyika?, *Freshw. Biol.*, 57(8), 1733–1744, doi:10.1111/j.1365-2427.2012.02828.x.
- Boer, F. De (2015), *HiHydroSoil: A high resolution soil map of hydraulic properties*, FutureWater report 134.
- Boschetti, L., D. Roy, and A. A. Hoffmann (2009), MODIS Collection 5 Burned Area Product-MCD45, *User's Guid. Ver, 2*.
- Cohen, A. S., M. R. Palacios-Fest, E. S. Msaky, S. R. Alin, B. McKee, C. M. O'Reilly, D. L. Dettman, H. Nkotagu, and K. E. Lezzar (2005), Paleolimnological investigations of anthropogenic environmental change in Lake Tanganyika: IX. Summary of paleorecords of environmental change and catchment deforestation at Lake Tanganyika and impacts on the Lake Tanganyika ecosystem, *J. Paleolimnol.*, 34(1), 125–145, doi:10.1007/s10933-005-2422-4.
- Cohen, M. J., M. T. Brown, and K. D. Shepherd (2006), Estimating the environmental costs of soil erosion at multiple scales in Kenya using emergy synthesis, *Agric. Ecosyst. Environ.*, 114(2-4), 249–269, doi:10.1016/j.agee.2005.10.021.
- Conaway, C. H., P. W. Swarzenski, and A. S. Cohen (2012), Recent paleorecords document rising mercury contamination in Lake Tanganyika, *Appl. Geochemistry*, 27(1), 352–359, doi:10.1016/j.apgeochem.2011.11.005.
- Donohue, I., and J. Garcia Molinos (2009), Impacts of increased sediment loads on the ecology of lakes., *Biol. Rev. Camb. Philos. Soc.*, 84(4), 517–31, doi:10.1111/j.1469-185X.2009.00081.x.
- Drake, N., M. Wooster, E. Symeonakis, and X. Zhang (1999), *Lake Tanganyika Biodiversity Project Special Study on Sediment Discharge and its Consequences: Soil Erosion Modeling in the Lake Tanganyika catchment*.
- Droogers, P., W. Terink, J. Brandsma, and W. W. Immerzeel. (2011), *Assessment of the Irrigation Potential in Burundi, Eastern DRC, Kenya, Rwanda, Southern Sudan, Tanzania and Uganda*, FutureWater Report 114.
- Eggermont, H., and D. Verschuren (2003), Impact of soil erosion in disturbed tributary drainages on the benthic invertebrate fauna of Lake Tanganyika, East Africa, *Biol. Conserv.*, 113(1), 99–109, doi:10.1016/S0006-3207(02)00353-1.
- Fang, X., D. B. Thompson, T. G. Cleveland, P. Pradhan, and R. Malla (2008), Time of Concentration Estimated Using Watershed Parameters Determined by Automated and Manual Methods, *J. Irrig. Drain. Eng.*, 134(2), 202–211, doi:10.1061/(ASCE)0733-9437(2008)134:2(202).



- Hunink, J. E., and P. Droogers (2015), *Impact Assessment of Investment Portfolios for Business Case Development of the Nairobi Water Fund in the Upper Tana River, Kenya*, Report FutureWater: 133.
- Hunink, J. E., P. Droogers, S. Kauffman, B. M. Mwaniki, and J. Bouma (2012), Quantitative simulation tools to analyze up- and downstream interactions of soil and water conservation measures: Supporting policy making in the Green Water Credits program of Kenya., *J. Environ. Manage.*, 111C, 187–194, doi:10.1016/j.jenvman.2012.07.022.
- Hunink, J. E., W. W. Immerzeel, and P. Droogers (2014), A High-resolution Precipitation 2-step mapping Procedure (HiP2P): Development and application to a tropical mountainous area, *Remote Sens. Environ.*, 140, 179–188, doi:10.1016/j.rse.2013.08.036.
- Immerzeel, W. W., L. P. H. van Beek, and M. F. P. Bierkens (2010), Climate change will affect the Asian water towers., *Science*, 328(5984), 1382–5, doi:10.1126/science.1183188.
- Itoh, N., M. Nakamura, H. Ihobe, S. Uehara, K. Zamma, L. Pintea, A. Seimon, and T. Nishida (2012), Long-term changes in the social and natural environments surrounding the chimpanzees of the Mahale Mountains National Park., *Deborah Patrick, St. Vincent Hosp. Indianapolis, Indiana, USA*, 211.
- Julian, J. P., and R. Torres (2006), Hydraulic erosion of cohesive riverbanks, *Geomorphology*, 76(1-2), 193–206, doi:10.1016/j.geomorph.2005.11.003.
- Lutz, A. F., W. W. Immerzeel, A. B. Shrestha, and M. F. P. Bierkens (2014), Consistent increase in High Asia's runoff due to increasing glacier melt and precipitation, *Nat. Clim. Chang.*, 4(7), doi:10.1038/NCLIMATE2237.
- Maruyama, A., M. Yuma, and B. Rusuwa (2011), Impacts of sedimentation on the abundance and diversity of cichlid fishes in Lake Malawi, in *Soil Erosion: Causes, Processes and Effects*, pp. 141–160, Nova Science Publishers, Inc.
- McIntyre, P. B., E. Michel, K. France, A. Rivers, P. Hakizimana, and A. S. Cohen (2005), Individual- and Assemblage-Level Effects of Anthropogenic Sedimentation on Snails in Lake Tanganyika, *Conserv. Biol.*, 19(1), 171–181, doi:10.1111/j.1523-1739.2005.00456.x.
- Neitsch, S. L., J. G. Arnold, J. R. Kiniry, J. R. Williams, and K. W. King (2005), Soil Water Assessment Tool (SWAT) Theoretical Documentation, *Blackl. Res. Center, Temple, TX*.
- Nkotagu, H., and K. Mbwambo (1999), *Lake Tanganyika Biodiversity Project Special Study on Sediment Discharge and its Consequences: Hydrology of selected watersheds along the lake Tanganyika shoreline*.
- O'Reilly, C. M., S. R. Alin, P.-D. Plisnier, A. S. Cohen, and B. A. McKee (2003), Climate change decreases aquatic ecosystem productivity of Lake Tanganyika, Africa., *Nature*, 424(6950), 766–8, doi:10.1038/nature01833.
- Odigie, K. O., A. S. Cohen, P. W. Swarzenski, and A. R. Flegal (2014), Using lead isotopes and trace element records from two contrasting Lake Tanganyika sediment cores to assess watershed – Lake exchange, *Appl. Geochemistry*, 51, 184–190, doi:10.1016/j.apgeochem.2014.10.007.
- Otu, M. K., P. Ramlal, P. Wilkinson, R. I. Hall, and R. E. Hecky (2011), Paleolimnological evidence of the effects of recent cultural eutrophication during the last 200years in Lake Malawi, East Africa, *J. Great Lakes Res.*, 37, 61–74, doi:10.1016/j.jglr.2010.09.009.



- Palacios-Fest, M. R., A. S. Cohen, K. Lezzar, L. Nahimana, and B. M. Tanner (2005), Paleolimnological investigations of anthropogenic environmental change in Lake Tanganyika: III. Physical stratigraphy and charcoal analysis, *J. Paleolimnol.*, 34(1), 31–49, doi:10.1007/s10933-005-2396-2.
- Patterson, G. (2000), *Lake Tanganyika Biodiversity Project Special Study on Sediment Discharge and its Consequences: Summary of findings.*
- Pelkey, N. (2000), Vegetation in Tanzania: assessing long term trends and effects of protection using satellite imagery, *Biol. Conserv.*, 94(3), 297–309, doi:10.1016/S0006-3207(99)00195-0.
- Ryan, C. M., and M. Williams (2011), How does fire intensity and frequency affect miombo woodland tree populations and biomass?, *Ecol. Appl.*, 21(1), 48–60, doi:10.1890/09-1489.1.
- Sileshi, G., F. K. Akinnifesi, O. C. Ajayi, S. Chakeredza, M. Kaonga, and P. W. Matakala (2007), Contributions of agroforestry to ecosystem services in the Miombo eco-region of eastern and southern Africa, *African J. Environ. Sci. Technol.*, 1(4), pp. 68–80.
- Sonneveld, B. G. J. ., and M. . Nearing (2003), A nonparametric/parametric analysis of the Universal Soil Loss Equation, *CATENA*, 52(1), 9–21, doi:10.1016/S0341-8162(02)00150-9.
- Van Steenberge, M. et al. (2011), A Recent Inventory of the Fishes of the North-Western and Central Western Coast of Lake Tanganyika (Democratic Republic Congo), *Acta Ichthyol. Piscat.*, 41(3), 201–214, doi:10.3750/AIP2011.41.3.08.
- Takeuchi, Y., H. Ochi, M. Kohda, D. Sinyinza, and M. Horii (2010), A 20-year census of a rocky littoral fish community in Lake Tanganyika, *Ecol. Freshw. Fish*, 19(2), 239–248, doi:10.1111/j.1600-0633.2010.00408.x.
- Tierney, J. E., M. T. Mayes, N. Meyer, C. Johnson, P. W. Swarzenski, A. S. Cohen, and J. M. Russell (2010), Late-twentieth-century warming in Lake Tanganyika unprecedented since AD 500, *Nat. Geosci.*, 3(6), 422–425, doi:10.1038/ngeo865.
- De Vente, J., and J. Poesen (2005), Predicting soil erosion and sediment yield at the basin scale: Scale issues and semi-quantitative models, *Earth-Science Rev.*, 71(1-2), 95–125, doi:10.1016/j.earscirev.2005.02.002.
- De Vente, J., J. Poesen, P. Bazzoffi, A. Van Rompaey, and G. Verstraeten (2006), Predicting catchment sediment yield in Mediterranean environments: the importance of sediment sources and connectivity in Italian drainage basins, *Earth Surf. Process. Landforms*, 31(8), 1017–1034, doi:10.1002/esp.1305.
- De Vente, J., J. Poesen, G. Govers, and C. Boix-Fayos (2009), The implications of data selection for regional erosion and sediment yield modelling, *Earth Surf. Process. Landforms*, 34(15), 1994–2007, doi:10.1002/esp.1884.
- Wang, G., P. Hapuarachchi, H. Ishidaira, A. S. Kiem, and K. Takeuchi (2008), Estimation of Soil Erosion and Sediment Yield During Individual Rainstorms at Catchment Scale, *Water Resour. Manag.*, 23(8), 1447–1465, doi:10.1007/s11269-008-9335-8.
- West, K. (2001), *Lake Tanganyika Biodiversity Project Special Study on Sediment Discharge and its Consequences: Results and Experiences.*



- Williams, J. . (1995), The EPIC model, in *Computer Models of Watershed Hydrology*, edited by V. P. Singh, pp. 909–1000., Colorado, USA.
- Williams, J. R. (1975), Sediment routing for agricultural watersheds, *J. Am. Water Resour. Assoc.*, 11(5), 965–974.
- Wischmeier, W. H. (1976), Use and misuse of the universal soil loss equation., *J. soil water Conserv.*, 31, 105–107.
- Wischmeier, W. H., and D. D. Smith (1978), *Predicting rainfall erosion losses - A guide to conservation planning.*, Agricultur., US Department of Agriculture, Washington, DC.
- WOCAT (2007), *Where the Land is Greener--Case Studies and Analysis of Soil and Water Conservation Initiatives Worldwide*, edited by H. Liniger and W. Critchley.
- Zhang, E., H. Tang, Y. Cao, P. Langdon, R. Wang, X. Yang, and J. Shen (2013), The effects of soil erosion on chironomid assemblages in Lugu Lake over the past 120 years, *Int. Rev. Hydrobiol.*, 98(3), 165–172, doi:10.1002/iroh.201301468.

